

LA-UR-11-11480

Approved for public release;
distribution is unlimited.

Title: Results from Seismic hazards Trench #1 (SHT-1)
Los Alamos Seismic Hazards Investigations

Author(s): Jamie N. Gardner
W.S. Baldrige
R. Gribble
Kim Manley
Kazuhiro Tanaka
John W. Geissman
Mark Gonzalez
_ _

Intended for:



Los Alamos National Laboratory, an affirmative action/equal opportunity employer, is operated by the Los Alamos National Security, LLC for the National Nuclear Security Administration of the U.S. Department of Energy under contract DE-AC52-06NA25396. By acceptance of this article, the publisher recognizes that the U.S. Government retains a nonexclusive, royalty-free license to publish or reproduce the published form of this contribution, or to allow others to do so, for U.S. Government purposes. Los Alamos National Laboratory requests that the publisher identify this article as work performed under the auspices of the U.S. Department of Energy. Los Alamos National Laboratory strongly supports academic freedom and a researcher's right to publish; as an institution, however, the Laboratory does not endorse the viewpoint of a publication or guarantee its technical correctness.

**RESULTS FROM
SEISMIC HAZARDS TRENCH # 1 (SHT-1)
LOS ALAMOS SEISMIC HAZARDS INVESTIGATIONS**

BY

**Jamie N. Gardner,¹ W. S. Baldrige,¹ R. Gribble,² Kim Manley,³
Kazuhiro Tanaka,⁴ John W. Geissman,⁵ Mark Gonzalez,² and Gregg Baron²**

Report No. EES1-SH90-19; December, 1990

1. Earth and Environmental Sciences, Los Alamos National Laboratory
2. Graduate Research Assistant, Los Alamos National Laboratory
3. Geological Consultant, 4691 Ridgeway Dr., Los Alamos, NM 87544
4. Central Research Institute of Electric Power Industry, 1646 Abiko City, Chiba, 270-11, JAPAN
5. Department of Geology, University of New Mexico



**LOS ALAMOS
NATIONAL LABORATORY**

JAN 13 1991

**LIBRARIES
PROPERTY**

CONTENTS

- I. Executive Summary
- II. Abstract
- III. Introduction and Background
- IV. Methods, Definitions, and Practical Considerations
 - A. Site selection
 - B. Excavation and restoration
 - C. Spatial control and logging
 - D. Stratigraphic units and sedimentological studies
 - E. Paleomagnetic studies
 - F. Carbon-14 dating
 - G. Definitions
- V. Geologic Setting
- VI. General Stratigraphy and Sedimentation
 - A. General description of stratigraphic units
 - B. Sedimentary compositions
 - C. Correlations
 - D. Depositional environments
- VII. Ages of Units
 - A. Constraints of geologic setting
 - B. Carbon-14 dates
 - C. Paleomagnetic constraints
 - D. Summary
- VIII. Structure
 - A. Main fault zone
 - B. Mid-trench low angle fault
 - C. Mid-trench strike slip zone
 - D. Ages and amounts of fault movements
 - E. Summary
- IX. Conclusions and Seismic Hazards Implications
- X. Acknowledgments
- XI. References

XII. Appendices

- A. Unit Descriptions
- B. Sedimentological data
 - 1. Granulometric data
 - 2. Clast Composition data
 - 3. Paleocurrent data

XIII. Pocket Contents

- A. Plate 1: Auger hole logs with correlative sections from the southwest wall of the main trench. Histograms of granulometric data.
- B. Plate 2: Reduction of 1:20 scale logs of the main trench.
- C. Plate 3: 1:10 scale log of main fault zone, northeast walls of main and slit trenches.
- D. Plate 4: 1:10 scale log of face of fault scarp in older portion of main fault zone.
- E. Plate 5: 1:10 scale log of southwest wall, main fault zone.
- F. Plate 6: 1988 1:10 scale log of northeast wall of slit trench (younger portion of main fault zone).
- G. Plate 7: 1988 1:10 scale log of part of southwest wall of slit trench (younger portion of main fault zone).
- H. Plate 8: 1:10 scale log of mid-trench low angle fault and strike slip zones; northeast wall of trench.
- I. Plate 9: 1:10 scale log of mid-trench strike slip zone on southwest wall of trench.

EXECUTIVE SUMMARY

Independent studies by the State of New Mexico and Los Alamos National Laboratory indicate that there is a potential for large, damaging earthquakes in the state. The New Mexico Bureau of Mines and Mineral Resources characterizes the earthquake potential and earthquake risk for Los Alamos County as high. Three active fault segments, each potentially capable of generating large earthquakes, have been identified in Los Alamos County. As part of the Laboratory's effort to quantify the hazard for each of these fault segments, a trench was excavated across one of the faults, the Guaje Mountain fault, in attempt to obtain information regarding the size, frequency, and last occurrence of earthquakes on this specific fault. Results from the trench studies indicate the Guaje Mountain fault typically generates earthquakes of Richter Magnitude 6.9 to 7.2. The most recent occurrence of one of these large earthquakes was between roughly 3700 and 6000 years ago. Attempts to determine the frequency of these earthquakes have not been successful, but similar faults near Albuquerque have been shown by other workers to generate such earthquakes every 6000 to 7500 years. Similar studies to those reported here will need to be done on each of the two remaining active fault segments in Los Alamos County to adequately quantify the local earthquake hazard and risk to the Laboratory.

ABSTRACT

Three active fault segments in Los Alamos County bear potential for generating large, damaging earthquakes. To quantify the seismic hazard to Los Alamos National Laboratory, we have begun to determine the parameters of the Characteristic Earthquake for each of these active fault segments. One of these fault segments, the Guaje Mountain fault, was trenched in attempt to obtain information on the size, frequency, and last occurrence of large earthquakes on the fault. Sedimentological studies of the deposits

exposed in the trench indicate the effects of faulting have influenced Quaternary drainage and sedimentation up through Holocene time. In addition, a major unconformity exists in the Quaternary record between greater than 730 ka and 6 ka. This unconformity may be regional, and was followed by a period of rapid aggradation between roughly 4000 and 3000 years ago that is very close in time to the youngest episode of faulting. At least three episodes of faulting can be identified in units with ages ranging from 5 Ma to 6 ka. Radiocarbon dates constrain the age of the youngest episode of faulting to between approximately 3700 and 6000 years ago. Net vertical slip during paleoseismic events appears to have been 1.5 to greater than 2 meters. Based on data presented by Slemmons (1977), these displacements occurred during Richter Magnitude 6.9 to 7.2 earthquakes. Attempts to determine the recurrence interval for these slip generating events have not been successful. However, Machette (1986) reports recurrence intervals of 6000 to 7500 years for similar faults near Albuquerque.

INTRODUCTION AND BACKGROUND

Historical perspectives, based on a relatively brief span of time, have fostered a false sense of security in the state of New Mexico with respect to earthquake hazards. In parallel studies between 1984 and 1985, personnel of the New Mexico Bureau of Mines and Mineral Resources and the Los Alamos National Laboratory sought answers to the question: is New Mexico, and for the one study more specifically Los Alamos County, at risk from potential earthquakes? (Johnpeer et al., 1986; Gardner and House, 1987). The answer to this question, in both independent studies, is an emphatic, albeit qualified, yes. Particularly within the corridor of the Rio Grande rift (Figure 1; see below) the New Mexico Bureau of Mines and Mineral Resources' position is that earthquake potential is high. Furthermore, Johnpeer et al. (1986) categorize the earthquake hazard and earthquake risk for Los Alamos

County as high. Gardner and House (1987) concluded that ample evidence existed to indicate that the faults in Los Alamos County must be considered capable of generating large, potentially damaging, earthquakes per the definitions of the Code of Federal Regulations. What, then, is the hazard? Just how big are these earthquakes? When was the last one and how likely is the next one? In the Los Alamos Seismic Hazards Program we are pursuing the answers to these questions for one specific area of New Mexico.

As part of Los Alamos National Laboratory's on-going program investigating seismic hazards in the Los Alamos County area, Seismic Hazards Trench # 1 (SHT-1; Figures 2 and 3) was excavated in 1987-1988 across the Guaje Mountain fault near the junction of Rendija and Cabra canyons. The objectives of the trenching were to create exposures in deposits younger than one million years in attempt to determine parameters of the Characteristic Earthquake for the Guaje Mountain fault segment of the Pajarito fault system (Figure 2; Gardner and House, 1987). Specifically, we sought to determine most recent movements, amount of movement per earthquake event, and the amount of time that elapsed between events.

The Guaje Mountain fault is one of a number of identified fault segments of the larger Pajarito fault system in the vicinity of Los Alamos (Figure 2). The Pajarito fault system constitutes the local active western boundary of deformation of the Rio Grande rift, a major continental tectonic feature, and has over 100 km of mapped fault traces (Gardner and House, 1987). Ample evidence exists to indicate that the Pajarito fault system is active or "capable" (Dames and Moore, 1972; Gardner and House, 1987; Wachs et al., 1988), and we believe, based on available data, that at least three of the identified fault segments within Los Alamos County bear potential for future earthquake activity.

To better quantify seismic hazards, and ultimately risks, to Los Alamos we seek information regarding the Characteristic Earthquake for each of these three fault segments. Other workers (for example, Schwartz and Coppersmith, 1984) have shown that fault segments generate similar-size large earthquakes with fairly regular periods of time between events. This earthquake model--the Characteristic Earthquake--is most useful in seismic risk studies because it provides an estimate of how frequently, the recurrence interval, a given size earthquake occurs on specific fault segments. Thus, the parameters of the Characteristic Earthquake taken together with information regarding the most recent movements allow fairly realistic estimates of the probability of a future large earthquake happening on a specific fault.

Some assumptions are fundamental in our approach. We assume that past fault movements have not been aseismic, but have been caused by earthquakes. In addition we assume that measurable fault parameters, such as amount of movement per event, can be related, based on world-wide empirical data, to the size of the earthquake (for example, Slemmons, 1977). These assumptions are conservative from a safety or hazards standpoint, and they are fundamental in paleoseismic analyses (for example, Slemmons, 1977; Schwartz and Coppersmith, 1984; Crone and Omdahl, 1987).

METHODS, DEFINITIONS, AND PRACTICAL CONSIDERATIONS

Site selection: The site for SHT-1 was selected for a number of reasons. Geologic mapping located the position of the fault trace, and an excellent exposure of the fault juxtaposing Bandelier Tuff and Tschicoma Formation dacite 70 meters north of the site (Figures 3 and 4). A number of geophysical studies in the area (Gardner and House, 1987; Wachs et al., 1988) and three auger holes (Figure 3 and Plate 1) indicated the area held promise for a thick sequence of young deposits within the fault zone. The site, within Los

Alamos County, is Department of Energy land, which made permitting and logistics relatively uncomplicated. Cultural resource and environmental action description surveys were conducted at the site. The actual position and orientation of the trench was dictated by the locations of trees and stream drainages.

Excavation and Restoration: The main trench was excavated with a front end loader. Excavation of the main trench took about three days in early July, 1987. Because of the remote possibility of encountering native American ruins and/or artifacts, an archaeologist was on site throughout most of the excavation and on call throughout the project. The topsoil of about the uppermost 0.3 to 0.5 meters was reserved separately from the rest of the spoil. The main trench was ramped from the surface on the northwest to about 4 meters deep on the southeast, about 70 meters long, and about 5 meters wide (Figure 3 and Plate 2). Although the deposits in which the trench was excavated were, for the most part, not lithified, the trench held near-vertical walls remarkably well. Barb-wire fences were erected around the excavation and appropriate hazard signs were displayed prominently. In addition, day-glow orange plastic visibility meshes were hung on the barb-wire fences. The land on which the trench was excavated belongs to the Department of Energy, but public access is unrestricted. In fall, 1987, a slit trench was excavated in the bottom of the southeastern end of the main trench with a backhoe. The ramped slit trench, about 8 meters long and one meter wide, exposed an additional two meters depth of the major fault trace (Figure 3 and Plate 2), and it too held near-vertical walls very well. While logging and assorted studies proceeded through the torrential rains of summer 1988, flooding in the slit trench became a problem. Periodically, the slit trench had to be pumped out, and it was re-excavated with a backhoe once. The trench was backfilled and compacted in fall 1988. The reserved topsoil was spread evenly over the filled excavation. The site was seeded with

grass and straw was spread to hold the seed and topsoil. Six pine saplings were planted on the fill. Today, except for the decomposing straw, there is no evidence in the field that the trench existed.

Spatial Control and Logging: An arbitrary datum for horizontal and vertical measurements was established near the shallow, northwestern end of the main trench (Figure 3). This datum was marked with spikes and flagging, and supplementary control marks were immediately surveyed and disguised so that spatial control could be re-established in case of vandalism. With a transit and/or surveyors level, the trench was mapped in plan, horizontal control points were marked with spikes and flagging at five meter intervals on the trench walls, and level lines were hung with nylon cord on spikes no more than five meters apart. Although the prime datum for spatial control survived the lifetime of the trench, severe vandalism did occur to markers and level lines within the trench, and re-surveying was necessary three times. The walls of the entire trench were logged at a scale of 1:20 (Plate 2) with measurements made from surveyed spatial control points or level lines with a tape or stadia rod. In like fashion, selected portions of structurally important zones were logged in greater detail at a scale of 1:10 (Plates 3 through 9). Attitudes of sedimentary structures, faults, fractures, and other features were measured with Brunton compass. The convention established for locations within the trench features symbols such as N35H, 3V; this symbol indicates a location on the northeast wall of the trench, 35 meters horizontally and 3 meters vertically down from the prime datum. An "S" instead of the "N" in the symbol would indicate a locality on the southwest wall. Because the slit trench was narrow and very close to the northeast wall, the "N" grid designation was used for locations on both walls of the slit trench.

Stratigraphic units and sedimentological studies: Stratigraphic units were defined in the walls of the trench on the basis of visible contacts, clast composition, textures, percentage of gravel, and induration. As they were defined the contacts of the units were etched with ice picks or masons trowels and color flagged to facilitate logging. Most units were given a letter designation as a name. There is no sequential or stratigraphic significance for the letter designation. The units consist mainly of stream, flood, and debris flow deposits and are each described in Appendix A. Where debris flows overlap each other, contacts were often difficult to distinguish. Because of this difficulty, the debris flow units as defined may well include deposits of more than one debris flow event. Each major stratigraphic unit was sampled at approximately 10 m intervals along the trench wall. Samples were field sieved for removal, weighing, and examination of the gravel fraction coarser than 4 mm. The remaining fraction, or split thereof, was sieved and weighed in the laboratory. Sample weights have been converted to weight percents and are given in Appendix B. In addition to gravel weight percent, the gravel fraction coarser than granule size has been described in several ways: 1) The coarsest clasts observed in the outcrop were measured and examined for composition, rounding, and sphericity. 2) The pebble and coarser fraction from field sieving was examined for overall composition of clasts and for size and composition of largest clasts. Estimates of the percentage of clasts of particular compositions were made. These data are given in Appendix B.

Flow direction indicators such as pebble imbrication, cross-bedding, and lag channel orientation were measured where possible. The information is listed in Appendix B, and shown in Figure 5.

Paleomagnetic studies: Samples were collected with a portable coring device or were manually cut as oriented blocks. Slightly lithified samples were impregnated. All

measurements were made on a 2G Enterprises, three measurement axis, 7.6 cm diameter horizontal access 760R superconducting rock magnetometer at the University of New Mexico. Details of alternating field and thermal demagnetization treatment, identification of magnetization components isolated in progressive demagnetization in the laboratory, and statistical evaluation of paleomagnetic data may be found in Geissman (1988).

Carbon-14 dating: ^{14}C dates were obtained by contract with Beta Analytic, Inc., in Coral Gables, Florida. This facility has an excellent reputation for both quality of data and rapid turn-around of results. Samples were prepared as follows: visual/microscopic examination for rootlets; acid, alkali, acid series of soakings to remove carbonate and humic acids; for most samples, benzene syntheses and beta counting; for very small samples, combustion with ensuing collection and purification of carbon dioxides; reaction of carbon dioxides with hydrogen on iron catalysts to produce graphite; application of graphite to copper targets with ensuing accelerator mass spectrometer measurements. Standard beta counts were for 24 hours. For smaller samples, extended beta counts were for four days to reduce statistical errors. Accelerator mass spectrometer measurements on extremely small samples were made in triplicate at the facility of the Eidgenossische Technische Hochschule University in Zurich. Dates are reported as radiocarbon years before 1950 A.D.; however, for the purposes of this report, the dates can be taken as years before the present or simply years ago. The half-life of radiocarbon is taken as 5568 years and 95% of the activity of the National Bureau of Standards Oxalic Acid (original batch) used as the modern standard. The stated errors are from the counting of the modern standard, background, and sample being analyzed; they represent one standard deviation statistics (68% probability), based on the random nature of the radioactive disintegration process. By international convention, no

corrections have been made for DeVries effect, reservoir effect, or isotopic fractionation in nature.

Definitions of selected terms as used in this report:

fracture: a tectonic break in rock or deposit without demonstrable movement or with ambiguous evidence for movement.

fault: a tectonic break in rock or deposit with evidence for movement. This evidence may include the presence of gouge or slickensides, development of planar or linear fabrics due to shearing and cataclasis, and/or offset stratigraphic markers. Faults can range from thin, sharp breaks, to wider bands of gouge, to even broader zones of shearing and brecciation. Generally the wider the zone of deformation becomes, the more likely we will refer to it as a fault zone.

main fault versus subsidiary fault: the fault with the greatest length, displacement, and/or surface continuity is taken to be the main fault for a particular episode of faulting. Subsidiary faults, also known as branch faults, are ruptures interpreted to be associated with major movements on the main fault and that either join the main fault at the surface or can be reasonably inferred to join it at depth. (usage of Bonilla, 1970).

fault contact versus depositional contact: a fault contact between units exhibits sharp, planar breaks in each unit, even in the absence of gouge or breccia. Most commonly, shearing is evident along fault contacts. In contrast, a depositional contact against a fault scarp will have a sharp boundary in the older, faulted unit, but a more diffuse boundary in the younger, unfaulted unit. Additionally, shearing will most commonly be present in the faulted unit and absent in the unfaulted one.

slickensides: grooves or striations generated within faults during movement.

Attitudes of slickensides and other linear fabrics developed during fault movement are reported herein as a trend and plunge.

gouge, breccia, sheared: these terms span a spectrum of textures that differ depending on extent or degree of cataclasis. A sheared rock or deposit usually exhibits intense fracturing with a pronounced planar fabric. A breccia consists of larger fragments set in a pulverized matrix. Gouge is material that has been totally pulverized to a paste.

Ma: this symbol means millions of years before present or millions of years ago.

ka: this symbol means thousands of years before present or thousands of years ago.

GEOLOGIC SETTING

The Rio Grande rift is a series of complex, asymmetric, fault-bounded basins extending from central Colorado to northern Mexico (Figure 1). Earliest extension in the rift began about 30 Ma; the present structures of the rift developed about 10 to 15 Ma (e.g., Chapin and Seager, 1975; Baldrige et al, 1980; Gardner and Goff, 1984; Seager et al., 1984). Arguably the rift is related to the Basin and Range tectonic province (Gardner and House, 1987). The Pajarito fault system is a generally north-trending swarm of normal to oblique-slip faults which form the active western boundary of the Española basin of the Rio Grande rift. Displacement on the main Pajarito fault is down to the east, toward the axis of the rift. In the vicinity of Los Alamos the main Pajarito fault exhibits individual scarps of 125 meters in rocks 1.13 Ma, and cumulative scarp heights in the same age rocks over 200 meters (Gardner and House, 1987; Goff et al., 1990). To the north, the Pajarito fault bends northeastward and merges with a northeast-trending system of faults called the Embudo fault zone (Aldrich, 1986).

Los Alamos and the Pajarito fault system lie on the eastern flanks of the Jemez volcanic field (Fig. 1; Smith et al., 1970). Voluminous volcanism began by about 13 Ma and accompanied structural development of the Española Basin (Gardner and Goff, 1984; Gardner et al., 1986). Two caldera-forming eruptions, 1.5 and 1.13 Ma, resulted in deposition of the Bandelier rhyolitic ignimbrite sheets (Smith et al., 1970; Spell et al., 1989). The Bandelier Tuff is a valuable reference horizon for determining the vertical component of offset along faults of the Pajarito system. Following formation of the 1.13 million year-old Valles caldera, eruption of rhyolitic tephra and lavas continued in the caldera until about 130,000 years ago (e.g., Gardner et al., 1986; Self et al., 1988).

GENERAL STRATIGRAPHY AND SEDIMENTATION

Generally, stratigraphy of the trench can be divided into three sequences, from youngest to oldest, as follows: units of the main trench, units of the slit trench, and units of the southeast end of the trench. Ages of units are discussed in the following section.

General description of units: The units of the main trench are dominantly debris flow and fluvial deposits. The fluvial units are sands, gravelly sands, and sandy gravels. They are not indurated, are grey to tan, and are commonly bedded in the sandier zones. Cross beds and cut and fill structures are common in these units. The gravel fraction of the fluvial units is generally pebble size, although cobble and boulder gravels are common as channel lags. The sand fraction is dominantly grains 1 to 0.5 mm in diameter. Only one fluvial unit (unit I) contains greater than 10% silt and clay. The debris flow units are brown to grey and are characterized by poor sorting, lack of induration, and lack of bedding or other sedimentary structures. Gravel clasts are supported in a sandy matrix. Most of these units, too, contain very low percentages of silt and clay size material; units B and H are the only debris flow units exposed in the trench with greater than 10% very fine-grained material.

The slit trench excavated in the bottom of the main trench near its southeastern end exposed an interbedded sequence of lacustrine clay beds and fluvial deposits. Separated from overlying deposits of the main trench by an angular unconformity, the slit trench deposits are lithified. Because of their intimate relations with the faulting, the slit trench units are described directly on the detailed 1:10 trench logs (Plates 6 and 7). These units received no letter designation and are referred to in discussions in the context of the slit trench.

The southeast end of the trench cut through and exposed several colluvial deposits which have been shed across the fault scarps. Compositionally, these colluvial units vary little and they consist of angular clasts of dacite in a clay rich arkosic sandy matrix. Three main colluvial units are distinguished, however, on the basis of position, induration, and structural relations. Colluvium I, oldest of the three, is well lithified and ubiquitously brecciated. Colluvium II is weakly lithified, and is draped across, and faulted within, the main fault zone (see below). Colluvium III is not indurated, and is interbedded with the fluvial-debris flow sequence of the main trench.

The southeast end of the trench exposed dacite bedrock on the upthrown block of the Guaje Mountain fault. The dacite is flow banded and is compositionally typical of the Tschicoma Formation of the Jemez volcanic field (see Smith et al., 1970, and Gardner et al., 1986). The dacite bedrock exposed in the trench is a part of a volcanic dome which forms Guaje Mountain. This dome is the local source for most of the dacite fragments and clasts found in younger units.

Sedimentary compositions: Gravel compositions in both fluvial and debris flow units are overwhelmingly dacite, pumice, and/or tuff. The composition of the sand fractions appears to be similar to the gravel with the addition of abundant mineral grains of quartz

and feldspar derived mainly from weathered pumice and tuff. The sands may best be described as lithic rich arkosic deposits. The percentage of dacite in the gravel fraction, relative to pumice and tuff clasts, is higher in almost all of the fluvial units than in the debris flows. Presumably, this is because the pumice and tuff clasts experience less abrasion and disaggregation during debris flow transport. Also apparently reflecting preservation during transport, charcoal was more abundant in debris flow deposits. Pumice clasts greatly outnumber tuff in all units. The largest clasts in all deposits are most commonly dacite. Units U, Colluvium II, and UU are the exceptions. In these units the largest clasts are tuff. Tuff and pumice clasts are generally more abundant in the granule and small pebble sizes than in larger sizes.

The dacite clasts are mostly very angular and the larger clasts are commonly disk-shaped with the short axis roughly 1/2 to 1/3 the length of the long. Tuff and pumice clasts are better rounded and commonly more spherical than the dacite. A few very well rounded dacite clasts suggest recycling from older alluvial units. One rounded small pebble of quartzite may have originally been a lithic fragment in one of the tuffs.

Correlations: Because of lateral discontinuities and abrupt facies changes, correlations of units between trench walls were commonly problematic. Generally, units could be easily traced in one wall of the trench, but some may anastomose in and out of exposure in the wall, resulting in unnecessary additional unit designation. These problems, however, do not affect structural or paleoseismic interpretations. Stratigraphic units considered equivalent on either side of the trench have been assigned the same letter designation. In the shallower, northwest half of the trench most of the units are correlative. To the southeast, however, correlation was much more difficult. Additional possible correlations include: S=SS; U=UU; J=b; D=t; and m=a (Plate 2).

Depositional environments: Current direction or flow indicators show that the direction of drainage has remained much the same as the present drainage (Figure 5). Flow in the northwestern half of the trench was to the east-southeast, and it appears that much of the Holocene section (i.e. units of the main trench), constrained by data on unit E, flowed around a small hill created by the faults bounding unit FF (see also Plates 8 and 9).

Deposits of the present intermittent stream in the drainage in the area of the trench are similar to those exposed in the trench walls with three exceptions. In contrast to the modern deposits, the trench units contain: 1) coarser gravel deposits, 2) better sorted gravel deposits, and 3) lacustrine deposits. These differences may reflect climate changes, a larger catchment area in the past, and/or changes in stream gradient or channel geometry.

Certainly the gravel textures in the trench indicate their transport by streams or rivers with much higher discharge rates than any seen today in the area. Coarse gravel deposition in fluvial systems tends to be immediately upstream from bends and constrictions (O'Connor et al., 1986; Lisle, 1986). The coarse gravels exposed in the trench are likely the result of both the bend and constriction in the drainage caused by a dam of erosion-resistant dacite bedrock upfaulted on the Guaje Mountain fault on the downstream side of the fault. Four thin beds of clay and thinly laminated siltstone exposed in the slit trench (Plates 6 and 7) are probably deposits of intermittent ponds or small lakes that formed with choking and damming of the drainage against the fault scarp.

The environment of deposition of most of the trench units appears to be one of intermittent storm-generated debris- and flood-flow deposits interspersed with periodic stream cut and fill activity. Similar environments are found on modern alluvial fans and particularly in areas of actively aggrading volcanoclastic wedges on the flanks of volcanoes. As mentioned above, charcoal is most abundant in the debris flow deposits. This relative

abundance is due in part to better preservation during transport, but may also indicate that many of the larger debris flows occurred as slurries triggered by storms following forest fires.

AGES OF UNITS

Ages of the units exposed in the trench are constrained by the geology of the surrounding area. Rendija Canyon, and its tributaries in the trench vicinity, are cut into units of the Bandelier Tuff and the Tschicoma formations. Tschicoma Formation dacite forming Guaje Mountain has been dated by K-Ar at 4.98 ± 0.15 Ma (Aldrich and Dethier, 1990). The Tshirege Member and the Cerro Toledo Rhyolite of the Bandelier Tuff formation have been dated by a variety of methods at 1.13 Ma and 1.5 to 1.20 Ma, respectively (Izett et al., 1981; Heiken et al., 1986; Spell et al., 1989).

Ten ^{14}C dates were obtained on charcoal samples from the trench by contract with Beta Analytic Inc., and are shown in Table 1 and on Plate 2. Most of these analyses were done on single pieces of charcoal, but a few were done on composite samples of millimeter-size charcoal flakes meticulously picked from individual units. It must be stressed that dating detrital material provides a maximum age for the sedimentary unit. Dates from composite samples could be hybrid, with potentially a variety of ages of charcoal from a unit being mixed together. The ^{14}C dates indicate that most of the alluvial units exposed in the trench are less than 6000 years old; furthermore, the dates suggest that the period of most significant aggradation in the drainage occurred between roughly 4000 and 3000 years ago when very large streams or rivers deposited thicknesses of sorted, extremely coarse gravels.

One apparent discrepancy between ^{14}C dates and stratigraphic relations has occurred. A composite sample from unit SS yielded a date of 4240 ± 80 years ago. However, unit SS appears to be stratigraphically younger than unit K which has a date on a single charcoal of 3730 ± 90 years ago. As pointed out above, dates on detrital material are maximum ages for

the sedimentary unit from which the detrital material came. Additionally, the date on the composite sample from unit SS could be on charcoal of a variety of ages. Thus, given these considerations and the stratigraphic relations, unit SS is no older than 4240 years, and is probably younger than 3730 years.

Paleomagnetic measurements constrain the age of the fluvial-lacustrine sequence exposed in the slit trench to greater than 730,000 years. The unit sampled was a fine-grained, light tan pumiceous sediment, 6-8 cm thick. Natural Remanent Magnetism directions of four samples had southerly declinations and shallow negative or positive inclinations. In progressive alternating field demagnetization, a steep, positive inclination magnetization of northerly declination was first removed in peak inductions up to 25 mT. This magnetization is probably a viscous remanent magnetization, acquired during the Brunhes chron (last 730 ka). At higher peak inductions, a southerly declination, moderate negative inclination magnetization was isolated. This higher coercivity magnetization is well-grouped and of reverse polarity, pointing essentially due south (Fig. 6). It is probably not a thermoremanent magnetization, since the ash and pumice fragments comprising this lithology were not deposited in water at temperatures above magnetite blocking temperatures (approximately 580°C). The magnetization may be a combination of a chemical remanent magnetization, acquired at moderate temperatures after ash deposition, and a depositional remanent magnetization reflecting field-driven orientation of fine magnetic particles. Regardless, this unit, barring an unusual self-reversing magnetochemical phenomenon, must have been deposited prior to 730,000 years ago. Because of structural juxtapositions, stratigraphic relations of this unit with others in the slit trench are not straightforward; however, it appears the paleomagnetically dated unit is older than unit colluvium II.

In summary, the oldest unit exposed in the trench is Tschicoma Formation dacite, about 4.9 Ma, on the upthrown fault block in the southeastern end of the trench. The oldest sedimentary deposits are greater than 730 ka. A major unconformity exists between greater than 730 ka and roughly 6 ka. The Holocene deposits in the trench appear to be younger than about 6 ka. A major period of aggradation occurred roughly between 4000 and 3000 years ago, with deposition of nearly 50 percent of the Holocene section. An additional significant period of aggradation may have occurred around 1600 years ago.

STRUCTURE

Three zones of deformation were exposed in the trench. For purposes of description, below, these zones are called: mid-trench strike-slip zone, mid-trench low angle fault, and main fault zone (see Plate 2). Interpretations of ages and amounts of movements are discussed in a later section.

Main fault zone: The main fault zone was exposed in the southeastern end of the trench from about N51H to about N63H in the northeast wall and slit trench, and from about S61H to about S66H in the southwest wall (Plates 3, 4, 5, 6, and 7). In general the exposed zone is over 10 meters wide and consists of two major fault traces, highly fractured deposits, cataclastically brecciated and sheared deposits, and subsidiary faults. We subdivide the main fault zone into two portions, older and younger, based on relative ages of movements.

The older portion of the main fault zone extends from N58.5H to about N63H (Plate 3). It contains one of the two major fault traces, mentioned above, which is most obviously expressed as a 1.5 to 2 meter scarp in dacite bedrock that cuts across the trench from N62.4H to S65.5H with an attitude of N8W, vertical. The face of the scarp is plastered with brecciated dacite and brecciated colluvium I (Plate 4). This scarp, and a highly fractured

and brecciated zone of dacite and colluvium I from N62.4 to about N58.5H, are overlain by largely undeformed colluvium II. On the southwest wall of the trench, this older portion of the fault zone is expressed only as a patch of brecciated colluvium I which abuts the scarp and is overlain by undeformed colluvium II (Plate 5). In addition to the major fault trace, two subsidiary faults are exposed in this area with attitudes of N22E, 81W, and N27E, 80SE. Most fractures are filled with amorphous silica in this portion of the main fault zone, and are parallel to sub-parallel to the three faults (Figure 7). Most slickensides plunge south; however, one set of slickensides on a subsidiary fault between N60H and N61H is near-horizontal, but plunges northeast.

The younger portion of the main fault zone was best exposed in the slit trench, from N51.5H to N58.5H, and in the southwest wall of the main trench around S62H (see Plates 3, 5, 6, and 7). The major fault trace at about N58H and S62H is a band of gouge, generally 10 to 15 cm thick, surrounded by sheared and cataclastically brecciated dacite and colluvium II. The fault, with an attitude of N9W, 74W, juxtaposes at least 2 meters of stratigraphic thickness of colluvium II on the west against shattered dacite on the east in the slit trench (Plates 3 and 6). In the southwest wall of the main trench colluvium II is on both sides of the fault (Plate 5). Thus, net vertical movement, consistent with mapped relations elsewhere along the fault (e.g., Gardner and House, 1987), has been down-to-the-west. A swarm of subsidiary faults exposed in the slit trench around N52H exhibit bands of gouge and, where discernible, small offsets of sedimentary units. Faults and fractures in this younger portion of the main fault zone are remarkably parallel and show a tight cluster of poles to their planes on the stereonet plot of Figure 7. Most faults in this area strike between north-south and about N10W. Slickensides throughout this portion of the main fault zone show plunges that range from horizontal, to the south, to vertical. Two sets of

slickensides, however, have shallow plunges to the north; one of these sets of slickensides is within the thick swath of gouge in the major fault trace. At the northwestern end of the slit trench the interbedded volcanoclastic sands and lacustrine silts and clay beds are tilted at about 20 to 30 degrees to the west with the strike of bedding parallel to faults and fractures (Plates 6 and 7). These relations may suggest that the tilting has been caused by faulting.

About 70 meters north of the trench the main fault zone is naturally exposed in outcrop in the steep arm of Cabra Canyon cut along the Guaje Mountain fault. A sketch of the outcrop, in which the fault juxtaposes Guaje Mountain dacite and non-welded Bandelier Tuff (Tshirege Member), is shown in Figure 4. The Bandelier Tuff exposed here is texturally identical to the large block included in colluvium II on the downthrown block of the younger portion of the main fault in the slit trench. In the natural exposure the fault is a zone of gouge and cataclastic dacite breccia about 10 cm wide, with an attitude of N20E, 86NW. Orientations of fractures and possible subsidiary faults are roughly parallel to the fault. The exposure is blanketed with a thin veneer of undeformed active colluvium.

The dominant sense of vertical movement in the main fault zone is down-to-the-west, based on juxtaposition of stratigraphic units in the slit trench and outcrop. This is consistent with how the fault zone has been mapped (e.g., Griggs, 1964; Smith et al., 1970, Gardner and House, 1987). Clearly, however, slickensides indicate an oblique slip component is common during movements. The orientations of most observed slickensides would require this oblique slip to be left lateral. The northerly plunging slickensides, on the other hand, would require a right lateral slip component. Left lateral slip has been recognized in some portions of the larger Pajarito fault system (Aldrich, 1986; Gardner and House, 1987; Reneau, unpub. data, 1990), but it is contrary to the right lateral

displacements that have been inferred for the Guaje Mountain fault segment (eg. Wachs et al., 1988).

Mid-trench low angle fault: The mid-trench low angle fault is exposed in the main trench at about N35.8H to N37.4H and S37H to S40H (Plates 2 and 8). The fault is a sharp break with an attitude of N11E, 50E. The fault is 1.5 to 2 cm wide and is infilled with amorphous silica and roots. Geometrically and spatially this fault appears to be subsidiary to the main fault zone, being parallel to and dipping into it, with associated fractures with orientations similar to those of the main fault zone (Figure 8). No slickensides were preserved in the low angle fault. The fault breaks unit FF in the northeast wall and is overlain by undeformed unit S. In the southwest wall the fault juxtaposes unit YY with the basal portion of unit FF, and is overlain by unfaulted unit SS. Net vertical movement on the fault is down-to-the-east.

Mid-trench strike-slip zone: The deformation in the midtrench strike-slip zone at N31H to N33H and S30H to S31.4H (Plates 8 and 9) has involved units FF, V, G, GG, and F. Foreset beds in unit G on the northeast wall have been abnormally steepened and dragged into the fault plane by the faulting; on the southwest wall the pebble gravel bedding has been truncated. The fault has an attitude of N83E, 44N. On the northeast wall of the trench, a block of unit FF, shattered with fractures and possible subsidiary faults that are all nearly parallel (Figure 9), sits above the sharp fault trace. The fault is 0.5 to 1.5 cm wide and is infilled with roots and amorphous silica. The dip of the fault plane is not constant, and, in fact, decreases dramatically towards the base of the logged trench exposure. Additional manual excavation into the floor of the trench (not logged) revealed that the fault flattens out completely into an underlying unconsolidated sand bed. A continuation of the fault trace was not found beneath the sand bed. Above the shattered block elongate pebbles

in unit F exhibit a pronounced alignment of N78E, 0 to 10W. This pebble alignment, parallel to the faults and fractures of this zone, is contrary to the flow directions of S68E measured in this unit away from the deformation. In the southwest wall of the trench the fault is a zone of intense shearing and brecciation that has created a foliated mixture of components derived from a number of units. The zone of this melange is up to 20 cm wide, and is oriented N80E, 50NW. Finger-like projections of unit V have been squeezed up in the shear zone to intrude overlying unit F. Undeformed unit P overlies this fault zone in both trench walls.

The flattening of the dip of the fault plane and translation of deformation along and through the unconsolidated sand bed would appear to require deformation in this zone to be pure strike-slip. Vertical to oblique movements should tend to create more vertically continuous fault traces and obliterate large deviations of fault plane dip, such as those observed. The pebble alignment and plunge strongly suggests that the shattered block, above the fault trace in the northeast trench wall, has been moved by left-lateral faulting. Lateral displacements of the shattered block, taken together with the abrupt facies changes of some units, can also explain how some lithologies in the block are continuous and correlative and some are not. The sense of deformation of the foreset pebble beds is also consistent with left slip, and the squeezed up digits of unit V in the southwest wall are indicative of at least localized compression during the strike-slip deformation.

Ages and amounts of fault movements:

The main fault zone exposed in the trench exhibits evidence for a minimum of three episodes of faulting. The variable orientations of slickensides may argue for more. Based on stratigraphic and structural constraints the three clear episodes of faulting are as follows: The fault scarp was created in the dacite at N62.4H and no doubt some of the brecciation,

shearing, and fracturing between N58.5H and N62.4H occurred in the oldest episode of faulting exposed. Following this episode of faulting, colluvium I was shed across the scarp and accumulated in topographic low spots in the breccia zone which was then exposed at the surface. A second episode of deformation cataclastically brecciated colluvium I and was in part responsible for fracturing, shearing, and brecciation between N58.5H and N62.4H. Additional episodes of deformation in this zone can not be discounted. Displacements of these earliest episodes are difficult to estimate, but net normal slip must have been at least 1.5 to 2 meters, the height of the dacite scarp. We have no control on the magnitude of horizontal or oblique slip. The only age constraints for these episodes of faulting are provided by the dacite age and the overlying undeformed colluvium II. Thus, these episodes of faulting occurred sometime between less than 4.98 Ma and greater than 3700 years ago. Following these earlier events, colluvium II was shed across the older portion of the main fault zone. Assuming a typical wedge shape for the colluvial deposit, colluvium II was faulted with greater than 2 meters of normal slip along the fault at N58H and S62H. It appears that preservation of a greater stratigraphic thickness of the toe of the colluvial wedge was favored by the downfaulting; much of colluvium II on the upthrown block has been eroded. These relations argue that most of the normal slip observed on colluvium II occurred at once, probably in one event. Had this not been the case, the greater stratigraphic thickness of the weakly lithified colluvial unit would not have been preserved in the drainage's channel. Again, although slickensides suggest a lateral or oblique component to the movements, the magnitude of this component can not be estimated. Age relations for this episode of faulting, independent of information from other faults in the trench, are provided by relations of colluvium II with the fluvial-lacustrine sequence of the slit trench and the overlying undeformed unit K. Thus, faulting occurred between roughly

700 ka and 3700 years ago. Subsidiary faults in the slit trench show orientations and age relations identical to the main fault at N58H; thus, we conclude these subsidiary faults formed during the same faulting event. The subsidiary faults mostly exhibit a few centimeters of vertical slip on stratigraphic markers. One subsidiary fault, however, at N51.8H in the southwest wall of the slit trench, shows a down-to-the-west sense of movement based on the dragging of several stratigraphic layers. This sense of movement, together with a lack of correlative layers on the opposite side of the fault, suggest net normal slip of at least 48 centimeters on this particular subsidiary fault.

The mid-trench low angle fault displays about one meter of normal slip, based on correlations of a sequence of subunits of unit FF across the fault in the northeast wall of the trench (N35.2H, 3.9V to 4.0V, and N36.5H, 4.2V to 4.4V; Plate 8). Here the fault is depositionally overlain by undeformed units S and P, containing charcoal dated at 3600 ± 170 years ago and 3495 ± 70 years ago, respectively. In the southwest wall of the trench the fault cuts the lower part of a sequence of debris flows, but appears to be depositionally overlain by the upper part of the sequence. Furthermore, charcoal from near the base of the sequence of debris flows yielded a ^{14}C date of 5690 ± 250 years ago, whereas charcoal from higher in the sequence gave a date of 4240 ± 80 years ago. As discussed above, resolution of contacts within packages of debris flows is difficult. Regardless, all of the debris flow sequence is non-indurated, and is therefore most probably of Holocene age. Thus, based on all available data, we have subdivided the debris flow sequence as shown on Plate 2; this, considering stratigraphic relations with unit K and considerations of ^{14}C dating of detrital material, very strongly suggests last movements on this fault occurred between 3730 ± 90 and 5690 ± 250 years ago. Given the geometric and spatial relations of the mid-trench low angle fault with the main fault zone, as well as youngest age constraints on deformation

discussed above and below, we believe this faulting represents deformation associated with the youngest movements on this segment of the Guaje Mountain fault.

The youngest units affected by deformation in the mid-trench strike slip zone are G and F. Undeformed unit P, containing charcoal dated at 3495 ± 70 years ago, overlies the zone in both walls of the trench. The youngest deformed units are unconsolidated, and are, therefore, probably Holocene in age; furthermore, they occupy the same stratigraphic position as units YY and SS. Thus, we conclude the deformation in the mid-trench strike slip zone occurred at the same time as that in the mid-trench low angle fault, between roughly 4000 and 6000 years ago. In that some sub-units of unit FF correlate and some do not across the strike slip fault and through the shattered block, we believe the amount of net left slip in this zone must be up to, but no more than, a few tens of centimeters. This magnitude of net slip is consistent with the dragging and smearing of the foreset pebble beds of unit G (Plate 8).

In summary, undeformed units on the order of 3500 to 3700 years old constrain the youngest limit of deformation everywhere in the trench. These relations alone argue strongly that the youngest episode of deformation in the main fault zone and the two mid-trench zones happened at the same time. Mid-trench deformation clearly has involved unconsolidated Holocene units. Our best interpretation of all available data indicates this youngest episode of faulting, throughout the trench exposures, occurred between roughly 3700 and 6000 years ago. Although there is clear evidence for multiple episodes of faulting exposed in the trench, we have been unsuccessful at dating, in any other than relative terms, the earlier episodes of deformation. However, on-going attempts to date material from fault gouge from the trench may yield additional constraints on other periods of movement. The amount of net normal slip per faulting event appears to have been typically 1 to 2 meters.

Horizontal components to the movements, although difficult to impossible to quantify, appear to have been small. Regardless, the estimates of net slip per event of 1 to 2 meters are minima.

CONCLUSIONS AND SEISMIC HAZARDS IMPLICATIONS

1) Effects of faulting have influenced the Quaternary drainage and sedimentation in the canyon up through Holocene time. These effects include lacustrine sedimentation in ponds behind the main fault; deposition of very coarse, sorted lag gravels at a bend and/or constriction in the drainage caused by an upfaulted block of erosion-resistant dacite; and, Holocene controls on paleocurrent flow directions by a fault block exposed in the mid-trench.

2) A major unconformity exists in the Quaternary sedimentary record between greater than 730 ka and about 6 ka. This is significant because the unconformity revealed in the trench represents a period of incision and non-deposition that is probably widespread. Thus, one would expect to find the same unconformity in most tributaries of the Pajarito Plateau drainage system.

3) A significant period of stream aggradation occurred between roughly 4000 and 3000 years ago. Greater than 50% of the Holocene section, all of which is less than 6000 years old, was deposited in this period of significant aggradation. The relations of this period of aggradation to youngest motions on the Guaje Mountain fault remain ambiguous, but the two events occurred very closely spaced in time.

4) At least three episodes of faulting are evident in dated units that range in age from 5 Ma to 6 ka.

5) Undeformed units on the order of 3500 to 3700 years old overlie all three zones of faulting exposed in the trench. Relations from the mid-trench faults indicate the youngest episode of faulting occurred between roughly 3700 and 6000 years ago.

6) Net vertical movements on the Guaje Mountain fault appear to have been 1.5 to greater than 2 meters per event. These estimates are minima in large part due to unconstrained quantities of horizontal to oblique slip.

7) As yet, no recurrence interval for these slip generating events has been determined for the Guaje Mountain fault.

Most of these conclusions have important bearing for seismic hazards in Los Alamos County. The Guaje Mountain fault clearly shows evidence of Holocene deformation, and is therefore an active fault. In the Code of Federal Regulations definitions, the Guaje Mountain fault is a "capable" fault, meaning that it must be considered capable of generating earthquakes. Based on relations presented by Slemmons (1977), the movements per event (1.5 to 2 meters) that we observed in the trench suggest Richter Magnitude 6.9 to 7.2 earthquakes have occurred in the past, and are expectable in the future. Although these earthquake estimates are probably minima, these values are consistent with those inferred for the Pajarito fault system by Gardner and House (1987). Additionally, the earthquake magnitude range we derive from the trench studies of the Guaje Mountain fault are similar (in fact virtually identical) to those determined by Machette (1986) for a similar fault system in the central Rio Grande rift near Albuquerque. For comparison, at least seven historical earthquakes with magnitudes greater than 7 have occurred in the tectonically related Basin and Range since 1871 (DuBois and Smith, 1980; Stein and Bucknam, 1985; Gardner and House, 1987). Assuming the entire surface expression of the Guaje Mountain fault, as shown in Gardner and House (1987), represents a rupture length of one earthquake event, other relations of Slemmons (1977) indicate an earthquake of Richter Magnitude 6.8 to 7.1 would have been responsible for the rupture. Thus, we conclude our estimates of magnitude

6.9 to 7.2, based on data from the trench, are good estimates of future expectable earthquakes on the Guaje Mountain fault.

Youngest movement, and therefore the most recent earthquake, on the Guaje Mountain fault appears to have occurred between about 4000 and 6000 years ago. Unfortunately, we have not yet had success in determining the recurrence interval for these earthquakes. Interestingly, Machette (1986) determined recurrence intervals for a similar fault system in the central Rio Grande rift near Albuquerque of 6000 to 7500 years.

ACKNOWLEDGEMENTS

A great many people have helped us in various ways. Dick Fox supervised the engineering of the trench and Jasper Tucker provided most of the highly skilled heavy equipment work. Bev Larson was the archeologist on the project and Teralene Foxx handled environmental concerns. We benefited greatly from the assistance and/or advice of a number of colleagues: Chuck Harrington, John Whitney, John Hawley, Steve Reneau, Dave Dethier, Larry Maassen, and Jim Aldrich to name a few. James Archuleta, Anthony Garcia, and Barb Hahn were champs in helping to pull together the final manuscript.

REFERENCES

- Aldrich, M. J., 1986, Tectonics of the Jemez lineament in the Jemez Mountains and Rio Grande rift; *J. Geophys. Res.*, 91, 1753-1762.
- Aldrich, M. J., and Dethier, D. P., 1990, Stratigraphic and tectonic evolution of the northern Española Basin, Rio Grande rift, New Mexico; *Geol. Soc. Am. Bull.*, 102, 1695-1705.
- Baldrige, W.S., Damon, P.E., Shafiqullah, M., and Bridwell, R.J., 1980, Evolution of the central Rio Grande rift, New Mexico: New potassium-argon ages; *Earth and Planet. Sci. Letters*, 51, 309-321.
- Bonilla, M.G., 1970, Surface faulting and related effects; in *Earthquake Engineering*, R.L. Wiegel, ed., Prentice-Hall, New Jersey, 47-74.
- Chapin, C.E., and Seager, W.R., 1975, Evolution of the Rio Grande rift in the Socorro and Las Cruces areas; *New Mexico Geological Soc. Guidebook* 26, 297-321.

- Crone, A.J., and Omdahl, E.M., (eds.), 1987, Directions in paleoseismology; U. S. Geological Survey, open-file report 87-673, 456 p.
- Dames and Moore, 1972, Report of geologic, foundation, hydrologic, and seismic investigation: Plutonium processing facility, Los Alamos Scientific Laboratory, Los Alamos, NM; Dames and Moore (Los Angeles, CA) Consulting Report, job number 0651-120-02.
- Dransfield, B.J., and Gardner, J.N., 1985, Subsurface geology of the Pajarito Plateau, Espanola Basin, New Mexico; Los Alamos National Laboratory report, LA-10455-MS, 15 p.
- DuBois, S.M., and Smith, A.W., 1980, The 1887 earthquake in San Bernardino Valley, Sonora; Arizona Bureau of Geology and Mineral Technology, Univ. Arizona, Spec. Paper 3, 112 p.
- Gardner, J.N., and Goff, F., 1984, Potassium-argon dates from the Jemez volcanic field: implications for tectonic activity in the north-central Rio Grande rift; New Mexico Geological Soc. Guidebook 35, 75-81.
- Gardner, J.N., Goff, F., Garcia, S., and Hagan, R., 1986, Stratigraphic relations and lithologic variations in the Jemez volcanic field, New Mexico; *J. Geophys. Res.*, 91, 1763-1778.
- Gardner J.N., and House, L., 1987, Seismic Hazards Investigations at Los Alamos National Laboratory, 1984 to 1985; Los Alamos National Laboratory Report, LA-11072-MS, 76 p.
- Geissman, J.W., 1988, Paleomagnetism and rock magnetism of Quaternary volcanic rocks and Late Paleozoic strata, VC-1 Core Hole, Valles caldera, New Mexico, with emphasis on remagnetization of Late Paleozoic strata; *J. Geophys. Res.*, 93, (B6), 6001-6025.
- Goff, F., Gardner, J.N., and Valentine, G., 1990, Geologic map of the St. Peters Dome area, Jemez Mountains, New Mexico; New Mexico Bureau of Mines and Mineral Resources, Map 69.
- Heiken, G., Goff, F., Stix, J., Tamanyu, S., Shafiqullah, M., Garcia, S., and Hagan, R., 1986, Intracaldera volcanic activity, Toledo caldera and embayment, Jemez Mountains, New Mexico; *J. Geophys. Res.*, 91, 1799-1815.
- Izett, G., Obradovich, J., Naeser, C., and Cebula, G., 1980, K-Ar and fission track zircon ages of Cerro Toledo rhyolite tephra units in the Jemez Mountains, New Mexico; U. S. Geol. Survey Prof. Paper, 1199, 37-41.
- Johnpeer, G.D., Love, D.W., and Hemingway, M., 1986, Assessment of earthquake hazards in New Mexico; Proc. Third National Conf. Earthquake Engineering; pp. 233-244.

- Lisle, T.E., 1986, Stabilization of a gravel channel by large streamside obstructions and bedrock bends, Jacoby Creek, northwestern California; *Geol. Soc. Am. Bull.*, 97, 999-1011.
- Machette, M.N., 1986, History of Quaternary offset and paleoseismicity along the La Jencia fault, central Rio Grande rift, New Mexico; *Bull. Seismological Soc. Am.*, 76, (1), 259-272.
- O'Connor, J.E., Webb, R.H., and Baker, V.R., 1986, Paleohydrology of pool and riffle pattern development, Boulder Creek, Utah; *Geol. Soc. Am. Bull.*, 97, 1-10.
- Schwartz, D.P., and Coppersmith, K.J., 1984, Fault behavior and characteristic earthquakes: Examples from the Wasatch and San Andreas fault zones; *J. Geophys. Res.*, 89, (B7), 5681-5698.
- Seager, W.R., Shafiqullah, M., Hawley, J.W., and Marvin, R., 1984, New K-Ar dates from basalts and the evolution of the southern Rio Grande rift; *Geol. Soc. Am. Bull.*, 93, 87-99.
- Self, S., Kircher, D.E., and Wolff, J.A., 1988, The El Cajete series, Valles caldera, New Mexico; *J. Geophys. Res.*, 93, 6113-6127.
- Slemmons, D.B., 1977, State-of-the-art for assessing earthquake hazards in the United States: Report 6, Faults and earthquake magnitude; U. S. Army Corps of Engineers, Waterways Experiment Station, Misc. Paper S-73-I, 129 p.
- Smith, R.L., Bailey, R.A., and Ross, C.S., 1970, Geologic map of the Jemez Mountains, New Mexico; U.S. Geological Survey, Misc. Geol. Investigations Map I-571.
- Spell, T.L., Harrison, M.T., and Wolff, J.A., 1989, Ar-Ar dating of the Bandelier Tuffs and associated ignimbrites: constraints on evolution of the Bandelier magma system; *EOS, Trans. Am. Geophys. Union*, 70, 1413.
- Stein, R.S., and Bucknam, R.C., 1985, The Basin and Range viewed from Borah Peak; *EOS, Trans. Am. Geophys. Union*, 66, 603.
- Wachs, D., Harrington, C.D., Gardner, J.N., and Maassen, L.W., 1988, Evidence of young fault movements on the Pajarito fault system in the area of Los Alamos, New Mexico; Los Alamos National Laboratory report, LA-11156-MS, 23 p.

APPENDIX A

UNIT DESCRIPTIONS

Units are listed in alphabetical order with double capital letters immediately following the same single letter and lower case letters listed at the end. The letter designations are arbitrary and do not indicate age or stratigraphic sequence. Descriptive names are assigned to the units using the classification system of Folk (1954). Symbols and significance of these names is as follows ("mud" includes silt and clay):

G= gravel: gravel fraction $\geq 80\%$
sG= sandy gravel: gravel $\geq 30 < 80\%$; sand/mud ratio 9:1
gS= gravelly sand: gravel $\geq 5 < 30\%$; sand/mud ratio 9:1
gmS= gravelly muddy sand: gravel $\geq 5 < 30\%$; sand/mud ratio between 1:1 and 9:1

Units are listed as either fluvial or debris flow. Colors given are from the standard Geological Society of America Rock-color Chart. No colors were assigned for units on the southwest wall.

Unit A. Debris Flow, 10YR6/2. This unit represents the soil zone which has developed on unit B. It is 10YR6/2 and varies from ~5 to 40 cm. Its contact with B is gradational. No sampling was done of this unit.

Unit B. Debris Flow, 10YR6/4, gS-gmS. Gradational basal contact with C throughout most of trench suggests the upper part of C was reworked and incorporated into B or that C is a flood flow unit that grades into a debris flow as a single contemporaneous deposit. Weakly indurated. Only samples from units H and I contain similar percentages of mud. Charcoal from this unit radiocarbon dated at 300 ± 70 years.

- Unit C. Fluvial, 10YR7/2, gS-sG. Predominantly a crystal-rich sand. Planar and cross bedding. Coarsest clasts in channels in lower part of unit. Max. channel depth on northeast = 75 cm. Upper contact gradational, lower contact erosional; channel at 35N cuts through D into top of E. Nonindurated, weathers as undercut.
- Unit D. Debris Flow, 10YR6/2, gS. Contains scattered pods of pumice. Both contacts erosional. Weakly indurated. Radiocarbon date on composite charcoal sample from this unit is 1610 ± 160 years.
- Unit E. Fluvial, 5YR8/1, sG-gS. Predominantly sandy gravel. Planar and cross bedding. At 39-40N contains 2 sequences fining upward from coarse pumice and dacite gravel to granules and very coarse crystal-rich sand. Includes lenses of pumice; one such lens at the top of unit was sampled separately (EE25N). Numerous small channels throughout unit in aggrading sequence. Channel depth 60 cm at 18N. Coarsest clasts not confined to channels. Upper contact erosional, lower contact both erosional and onlapping. Nonindurated but holds cliff.
- Unit F. Debris Flow, 10YR7/2, sG-gS. Predominantly sandy gravel containing pods of pumice that provide faint bedding. Lower contact mainly depositional, upper erosional. Weakly indurated.
- Unit FF. Debris Flow, 10YR7/2, sG-gS. Improperly sampled and originally logged as a single unit. Subdivided and described in greater detail on 1:10 scale log shown in Plate 8. Contains multiple debris flows, bedded arkosic sands, and pumiceous sands and gravels. Well indurated. Upper contact erosional, lower depositional on GG. Unit is apparently much older than all other units of the main trench; possibly correlative to the fluvial-lacustrine sequence of the slit trench.

- Unit G. Fluvial, 5Y7/1, sG. Planar and cross bedding; foreset beds of small pebbles have been rotated by mid-trench faulting. Contacts depositional. Weakly indurated.
- Unit GG. Fluvial, gS. Planar bedding. Upper contact depositional, lower not exposed. Weakly indurated.
- Unit H. Debris Flow, gmS. Contains pumice pods. Gravel lens at 50S. Upper contact erosional, lower mainly erosional. Weakly indurated.
- Unit HH. Debris Flow, gS. Contacts mainly erosional. Weakly indurated. Contains finely disseminated charcoal that yielded a radiocarbon date of 3800 ± 100 years.
- Unit I. Fluvial, gmS. Faint planar bedding. Upper contact erosional, lower depositional. Weakly indurated.
- Unit J. Fluvial, sG. Small pebble gravel. Planar bedding. Contacts erosional. Nonindurated.
- Unit JJ. Fluvial, sG. Very poorly sorted. Faint bedding. Pumice pods. Small channel of sand near S55H. Contacts erosional. Nonindurated.
- Unit K. Fluvial, 10YR6/2, gS-sG. Planar and cross bedding. Gravel fraction appears to coarsen to southeast. Two large clasts (25 and 37 cm) at S53.5H. Contains many large channels (greater than 1 meter deep). Nonindurated but holds cliff. Radiocarbon date on charcoal from this unit is 3730 ± 90 years.
- Unit L. Fluvial, gS. Predominantly small pebble gravel. Max. exposed clast = 5 cm. Planar bedding in sandy parts. Contacts erosional. Nonindurated.
- Unit M. Fluvial, gS. Faint bedding. Fines upward but contains internal channels. Finer with more visible planar bedding to northwest. Max. exposed clast = 15 cm.

- Ends to southeast in depositional contact against well-indurated colluvial unit.
- Contacts mainly erosional. Nonindurated.
- Unit N. Fluvial, sG. Coarse pebble gravel. Fines upward to pebbly, very coarse sand. Planar bedding in sandy parts. Max. exposed clast = 18 cm. Some clasts are moderately well rounded. In depositional contact with indurated colluvial unit II at southeast end of trench.
- Unit P. Debris Flow, 10YR6/2, gS. Contacts mainly erosional. Weakly indurated. Composite charcoal sample has radiocarbon age of 3495 ± 70 years.
- Unit R. Fluvial, 10YR6/2, sG. Poorly sorted pebble gravel. Erosional contacts. Nonindurated.
- Unit S. Debris Flow, 10YR6/2, gS. Erosional contacts. Weakly indurated. Composite charcoal sample has radiocarbon age of 3600 ± 170 years.
- Unit SS. Debris Flow, gS. Max. exposed clast = 7 cm. Upper contact erosional, lower depositional and gradational. Weakly indurated. Composite charcoal sample has radiocarbon age of 4240 ± 80 years.
- Unit T. Fluvial, 5YR7/1, sG. Poorly sorted. Lacks bedding except for one small internal channel. Contacts erosional. Nonindurated.
- Unit U. Debris Flow, 10YR7/2, sG-gS. Pebbles slightly concentrated at base. Pumice pod at base from N44.5H to N45H. Numerous large pumice pebbles. Lower contacts mainly depositional, upper erosional. Weakly indurated.
- Unit UU. Debris Flow, gS. Numerous pumice pebbles. Max. exposed clast = 8 cm. Contacts mainly erosional. Weakly indurated. Two charcoal samples gave radiocarbon ages of 2840 ± 75 and 2970 ± 100 years.

Unit V. Debris Flow, 10YR7/4, gS. Upper contact depositional, lower not exposed.

Moderately indurated.

Unit W. Debris Flow, 10YR7/3, gS. Some stacked gravel clasts. Lower contact

depositional, upper erosional. Weakly indurated.

Unit Y. Debris Flow, gS. Max. exposed clast = 4.5 cm. Contacts erosional. Weakly

indurated.

Unit YY. Debris Flow, gS. Upper contacts gradational. Radiocarbon date on charcoal

from this unit is 5690 ± 250 years.

Unit Z. Fluvial, 10YR6/2, gS. Planar and cross bedding. Minor channels. Coarsens to

southeast. Clasts >5 cm until unit merges with, and becomes indistinguishable

from, K. Contacts erosional. Nonindurated.

Unit ZZ. Fluvial, sG. Faint planar bedding in sandy parts. Max. exposed clast = 20

cm. Pod of small pumice pebbles near base. Contacts erosional. Nonindurated.

Unit a. Fluvial, N7 & 10YR7/2, sG. Lacks bedding. Contacts erosional,

Nonindurated.

Unit b. Fluvial, 5YR7/1, sG. Planar bedding in sandy parts. Coarsens to southeast.

Max exposed clast = 10 cm. Deposited against nonindurated colluvial unit on northeast.

Unit g. Fluvial, N7 & 10YR7/2, sG. Faint planar bedding near top in sandy part.

Max. exposed clast = 15 cm. Depositional against well-indurated colluvial unit; appears to underlie nonindurated colluvial. Contacts mainly erosional.

Nonindurated.

Unit t. Debris Flow, 5YR7/1, gS. Coarsest clasts near base. Max. exposed clast = 6 cm.

Similar pebbles float throughout unit. Depositional against nonindurated colluvium III.

Unit x. Fluvial, N7 & 10YR7/2, sG. Faint bedding in predominantly small pebble gravel. Max. exposed clast = 20 cm. Depositional against well-indurated colluvium II. Contacts mainly erosional. Nonindurated.

Colluvium I. Original textures of this unit have been obliterated by brecciation in the main fault zone. The unit is light orange to grey and occurs as shattered remnants of a colluvial wedge that once covered the main fault in dacite. The unit is well lithified and consists of seriate fragments of dacite in a clay-rich matrix.

Colluvium II. Massive, non-sorted, orange deposit of mostly dacite clasts in a clay-rich sandy matrix. Clasts range up to one meter. Contains sparse blocks of Bandelier Tuff. Moderately to well indurated. Overlies colluvium I and brecciated dacite, but is mostly undeformed by the the events that brecciated colluvium I.

Colluvium III. Non-indurated, massive grey to light orange, non-sorted deposit of mostly dacite blocks in a sandy matrix. Clasts range to one meter. Contains sparse fragments of Bandelier Tuff. Interfingers with Holocene fluvial and debris flow units of the main trench.

Fluvial-lacustrine sequence of the slit trench. Interbedded white to tan arkosic arenite and thin (about 3 to 5 cm) dark grey clay beds. Arenites exhibit normal grading. Locally tuffaceous. Units are lithified and tilted. Upper contact with Holocene units of the main trench is an angular unconformity. Samples of siltstone from this unit have reversed magnetic polarity, and are, therefore, greater than 730,000 years old.

BLANK PAGE

APPENDIX B: SEDIMENTOLOGICAL DATA

Part 1: Granulometric data

Samples have been given a combination letter-number-letter designation. The first letter represents the stratigraphic unit, the number represents the horizontal location in meters, and the last letter indicates whether the sample was from the northeast or southwest wall.

Samples are listed alphabetically with double letters following single, lower case letters following capital, and southwest wall samples following northeast wall.

Letters given below sample numbers indicate word descriptions of the units following the system described under Appendix A.

Size fractions are given using the phi scale. Gravel = >2 , sand = $<2 >4$, mud (silt and clay) = <4 .

SIZE	SAMPLE	WT. %	SAMPLE	WT. %	SAMPLE	WT. %
>-2	B15N	12	B25N	15	B35N	11
>-1		5		8		6
>0	gS	14	gmS	12	gmS	20
>1		19		14		26
>2		17		14		16
>3		13		13		10
>4		10		12		8
<4		9		13		6
TOTAL		99		101		100

SIZE	SAMPLE	WT. %	SAMPLE	WT. %	SAMPLE	WT. %
>-2	B45N	11	B55N	7	B30S	3
>-1		5		6		6
>0	gS	18	gmS	14	gmS	15
>1		29		19		18
>2		19		15		16
>3		7		12		14
>4		5		12		15

<4		5		16		11
TOTAL		99		101		98
SIZE		SAMPLE WT. %		SAMPLE WT. %		SAMPLE WT. %
>-2	C15N	14	C25N	5	C35N	33
>-1		9		5		7
>0	gS	36	gS	27	sG	23
>1		30		38		23
>2		9		18		9
>3		2		4		2
>4		1		1		0.9
<4		1		1		1
TOTAL		102		99		98.9

SIZE		SAMPLE WT. %		SAMPLE WT. %		SAMPLE WT. %
>-2	C45N	9	C55N	19	C30S	5
>-1		7		10		5
>0	gS	31	gS	31	gS	24
>1		33		26		32
>2		13		8		19
>3		3		2		7
>4		2		0.9		4
<4		2		2		4
TOTAL		100		98.9		100

SIZE		SAMPLE WT. %		SAMPLE WT. %		SAMPLE WT. %
>-2	D15N	11	D25N	11	D34N	12
>-1		6		7		7
>0	gS	19	gS	17	gS	13
>1		20		20		19
>2		15		18		20
>3		11		11		13
>4		11		8		9
<4		8		9		8
TOTAL		101		101		101

SIZE		SAMPLE WT. %		SAMPLE WT. %		SAMPLE WT. %
>-2	D45N	13	DD30S	50	E15N	24
>-1		6		6		7
>0	gS	21	sG	11	sG	25
>1		27		10		28
>2		18		7		11
>3		8		5		3
>4		4		4		1
<4		4		6		2

TOTAL		101		99		101
SIZE		SAMPLE WT. %		SAMPLE WT. %		SAMPLE WT. %
>-2	E25N	32	E35N	25	E45N	16
>-1		7		7		8
>0	sG	25	sG	25	gS	30
>1		23		28		31
>2		8		10		10
>3		2		3		2
>4		1		1		0.9
<4		1		0.7		1
TOTAL		99		99.7		98.9

SIZE		SAMPLE WT. %		SAMPLE WT. %		SAMPLE WT. %
>-2	E30S	57	EE25N	22	F25N	31
>-1		10		7		11
>0	sG	17	gS	29	sG	12
>1		11		22		15
>2		14		11		16
>3		1		3		9
>4		0.5		1		3
<4		0.1		2		2
TOTAL		100.6		97		99

SIZE		SAMPLE WT. %		SAMPLE WT. %		SAMPLE WT. %
>-2	F30N	33	F30S	14	FF35N	27
>-1		8		9		6
>0	sG	12	gS	18	sG	15
>1		14		22		21
>2		14		17		13
>3		9		12		11
>4		6		5		6
<4		4		3		1
TOTAL		100		100		100

SIZE		SAMPLE WT. %		SAMPLE WT. %		SAMPLE WT. %
>-2	FF40N	14	FF35S	11	G25N	52
>-1		10		7		10
>0	gS	26	gS	19	sG	20
>1		24		25		12
>2		11		15		3
>3		5		10		2
>4		4		7		0.2
<4		4		6		0.2
TOTAL		98		100		99.4

SIZE	SAMPLE WT. %		SAMPLE WT. %		SAMPLE WT. %	
>-2	G30N	39	G30S	42	GG37S	9
>-1		20		22		4
>0	sG	29	sG	21	gS	21
>1		10		7		31
>2		2		4		19
>3		0.3		2		9
>4		0.2		0.9		4
<4		0.4		0.6		2
TOTAL		100.9		99.5		99

SIZE	SAMPLE WT. %		SAMPLE WT. %		SAMPLE WT. %	
>-2	H45S	11	HH40S	18	I35S	8
>-1		3		6		9
>0	gmS	9	gS	14	gmS	21
>1		16		18		25
>2		19		15		12
>3		17		12		4
>4		12		11		2
<4		12		6		17
TOTAL		99		100		98

SIZE	SAMPLE WT. %		SAMPLE WT. %		SAMPLE WT. %	
>-2	J57S	43	JJ56S	43	K45N	4
>-1		4		10		4
>0	sG	16	sG	20	gS	28
>1		22		16		41
>2		10		6		17
>3		2		2		4
>4		0.9		1		1
<4		0.8		1		1
TOTAL		98.79		9		100

SIZE	SAMPLE WT. %		SAMPLE WT. %		SAMPLE WT. %	
>-2	K55N	39	K50S	16	L61S	16
>-1		10		10		7
>0	sG	27	gS	30	gS	27
>1		18		27		32
>2		4		11		13
>3		1		3		2
>4		0.8		2		0.8
<4		0.7		1		0.9
TOTAL		100.5		100		98.7

SIZE	SAMPLE WT. %		SAMPLE WT. %		SAMPLE WT. %	
>-2	M57S	2	N61S	74	P25N	10
>-1		5		6		9
>0	gS	30	sG	11	gS	16
>1		37		6		18
>2		17		1		16
>3		5		0.3		10
>4		2		0.1		11
<4		1		0.2		9
TOTAL		99		98.6		99

SIZE	SAMPLE WT. %		SAMPLE WT. %		SAMPLE WT. %	
>-2	P35N	12	R40N	47	S37N	13
>-1		5		5		6
>0	gS	12	sG	9	gS	16
>1		19		11		22
>2		18		11		16
>3		16		8		11
>4		13		6		8
<4		4		3		8
TOTAL		99		100		100

SIZE	SAMPLE WT. %		SAMPLE WT. %		SAMPLE WT. %	
>-2	S40N	8	SS40S	7	T43N	29
>-1		7		6		9
>0	gS	13	gS	16	sG	34
>1		18		24		20
>2		18		18		5
>3		15		13		1
>4		12		11		0.6
<4		8		6		1
TOTAL		99		101		99.6

SIZE	SAMPLE WT. %		SAMPLE WT. %		SAMPLE WT. %	
>-2	U45N	26	U50N*	22	UU45S	12
>-1		9		7		8
>0	sG	18	gS	14	gS	10
>1		19		18		15
>2		11		15		18
>3		6		10		15
>4		5		7		14
<4		5		8		9
TOTAL		99		101		101

SIZE	SAMPLE WT. %		SAMPLE WT. %		SAMPLE WT. %	
------	--------------	--	--------------	--	--------------	--

>-2	V28N	6	W33N	10	W34N	8
>-1		9		7		6
>0	gS	24	gS	21	gS	20
>1		28		27		26
>2		16		16		16
>3		8		9		10
>4		5		7		8
<4		3		4		6
TOTAL		99		101		100

SIZE	SAMPLE WT. %	SAMPLE WT. %	SAMPLE WT. %	WT. %		
>-2	Y45S	10	Z45N	15	ZZ45S	41
>-1		9		7		11
>0	gS	10	gS	26	sG	17
>1		13		33		15
>2		16		13		8
>3		18		3		4
>4		16		1		2
<4		8		2		2
TOTAL		100		100		100

SIZE	SAMPLE WT. %	SAMPLE WT. %	SAMPLE WT. %	WT. %		
>-2	a55N	52	b58N	21	g55N	61
>-1		7		11		7
>0	sG	13	sG	33	sG	15
>1		14		23		11
>2		8		7		3
>3		3		2		1
>4		1		0.8		0.5
<4		3		1		0.8
TOTAL		101		98.8		99.3

SIZE	SAMPLE WT. %	SAMPLE WT. %	SAMPLE WT. %	WT. %		
>-2	t59N	27	x57N	64	*UU35S	8
>-1		7		6		6
>0	gS	21	sG	16	gS	15
>1		21		10		25
>2		11		2		24
>3		6		0.4		12
>4		3		0.1		6
<4		3		0.3		4
TOTAL		99		98.8		100

PART 2: CLAST DATA

DATA ON GRAVEL FRACTION LESS GRANULES

Measurements in cm of maximum length (a axis) were made on several pebbles, cobbles, and boulders from each major unit exposed in the northeast wall (EML). These clasts were also described in terms of composition (COMP), roundness (R), and sphericity (S). The last two measurements are recorded here as whole numbers for convenience but should be read as tenths. Locations of clasts are given in meters horizontally (LOC H) and vertically (LOC V) from the datum. Compositions are predominantly dacite (d), pumice (p), and tuff (t). Other clasts include unidentified volcanic rocks (v), obsidian (o), glassy dacite (g), and scoria (s). Maximum exposed clast size was noted for only some of the units of the southwest wall.

UNIT	EML	COMP	R	S	LOC H	LOC V
B	5	d	7	3	12.2	1.2
	3.2	d	3	5	24.8	1.5
	2.2	t	7	6	15.3	1.4
C	15.2	d	7	7	5	3
	30.5	d	3	9	18.6	2
	23	d	3	8	19.9	1.9
	29	d	1	5	22.5	2
	10.5	d	3	5	32	1.9
	12.7	d	7	7	34.2	2.4
	13	d	2	3	34.2	2.5
	16.5	d	4	3	38.9	3
	7	d	1	3	44.7	3.1
	11.5	v	1	3	47.5	2.6
D	4.5	t	7	7	11.1	2.2
	4	t	7	6	12.3	2.3
	6	t	6	5	16	2.1
	6	d	2	7	17.2	2.4
	10	d	2	5	28.9	2.8
	9.5	t	1	3	30.1	2.3
	5.7	t	1	2	36	3.2
	8.5	d	2	7	36.9	3
	10	d	7	8	45.6	3.3
	20	d	1	6	49	3.5
E	21.5	v	7	7	15	3
	21.5	d	5	9	20.3	2.7
	16.5	d	2	4	18.6	3.6
	10	v	7	7	22	5.2
	19	d	2	5	23.3	3.6
	20.3	d	5	7	25.6	3

Report No. EES1-SH90-19
December 1990

	14.5	d	2	4	29.3	3.3
	15	t	7	8	37.3	3.5
	25.5	d	5	9	40	3.5
	18	d	3	7	42.5	3.7
	25.5	d	1	7	49.2	2.9
F	6.5	d	2	7	24	4.5
	3.5	t	3	7	27.4	4.4
	4	d	5	5	27.3	4.4
	4.5	t	9	7	27.9	4.3
	4	t	9	7	30.8	4.5
	2	d	1	6	33	4.2
	4	d	1	5	34.9	4.2
	6.5	d	1	7	35.5	4.3
	3.5	0	1	6	35.5	4.3
	3	d	1	6	37	4.7
G	4.5	d	2	4	29.2	4.8
	4.5	d	2	3	29.2	4.8
	4.5	d	3	4	29.3	4.9
	4	d	2	4	29.3	4.9
	8	t	7	7	29.3	4.9
	3.5	d	3	3	29.3	5
	6.5	d	1	2	29.3	5
	3.5	d	8	3	29.4	4.8
	6	d	6	6	29.4	4.8
	5	d	2	6	29.4	4.9
J	2	d				
JJ	13	d				
K	5	d	5	3	47	4.8
	13	d	6	3	48.4	4.7
	37	d			53.5S	
	25	d			53.5S	
L	5	d				
M	15	d				
N	18	d				
P	4	d	3	7	24.3	3.9
	4	r	9	8	29.9	4.1
	3	t	7	5	30	4
	3	d	2	7	32.5	3.2
	7	d	2	8	35.5	3.8
	6	t	7	7	36.1	3.9
	5.5	d	1	8	36.2	3.8

	3.5	t	1	7	37.9	4.2
	5	t	5	6	38.5	4.1
	6	d	8	7	40.3	4.2
R	20	d	1	3	39.3	4.4
	9	d	4	3	40	4.5
	6.5	d	2	6	40.2	4.5
	7	d	1	3	40.4	4.4
	9	d	2	7	40.7	4.5
	4	d	5	7	41.3	4.5
	7.5	d	5	7	41.4	4.5
	6.5	t	9	5	42.1	4.5
	9	d	3	5	42.1	4.5
	8	v	8	7	42.1	4.5
S	6.5	d	1	6	36.6	4.2
	3.5	d	3	7	36.7	4.1
	15	t	8	9	37.7	4.7
	5.5	t	7	7	38.5	4.6
	4.5	d	4	3	38.5	4.9
SS	7	d				
T	8	d	1	7	43	4.3
	7.5	d	3	4	43.6	4.4
	5.5	d	1	4	43.6	4.4
	6.2	d	5	3	44	4.5
	18	t	7	8	44.2	4.5
U	8.5	t	7	5	44.5	4.1
	10	t	7	7	44.7	4.1
	8	d	1	7	45.2	4.2
	13	t	6	8	45.5	4.2
	18	t	9	9	45.6	4.2
	11.5	t	8	3	46.2	4.3
	10	t	8	5	46.7	4.1
	11.5	d	2	8	47.7	4.2
	27	t	9	7	48.9	4.3
	10.5	d	1	7	50.2	4.4
UU	8	p				
V	1.5	d	3	4	27.6	4.8
	2	d	1	7	27.8	4.9
	1.5	d	5	9	28.4	4.9
	1	t	5	7	27.6	4.8
	1.5	d	2	5	27.7	4.9
W	3.5	d	1	7	33.2	3.8
	3	d	5	8	33.7	3.9

Report No. EES1-SH90-19
December 1990

	78	d	1	7	34.2	3.8
	4	d	1	3	34.4	4
	3	d	1	3	32.8	4
Y	4.5	t				
	4	d				
ZZ	19	d				
	19	d				
	20	d				
a	16	t	8	8	54	3.8
	14	d	1	7	56	4
b	10	d				
g	15	d				
t	6	d				
x	20	d				

The gravel fraction (less granules) was examined from each sieved channel sample. The maximum length of the three largest was measured in cm (ML) and their composition noted (COMP). Estimates were made of the overall composition of this gravel fraction (SIEVED COMP %).

SAMPLE	SIEVED COMP. %	ML	COMP.
B15N	70 d	5	d
	28 t/p	4.5	t
	2 s	4	d
B25N	90 t/p	4	d
	10 d	4	d
		3.8 t	3.8 d
B35N	85 t	3	d
	15 d	3	t
		2.5	p
		2.5	d
B45N	50 t	4	d
	50 d	3.5	d
		2.5	d
B55N	95 t/p	3	d
	5 d	2.6	d
		2	t
B30S	90 t/p	2.6	t
	10 d	2.5	p
		2.3	p
C15N	90 d	5.5	d
	10 t/p	4.5	t
		3.5	d
C25N	60 d	4	d
	40 t/p	4	d
	2.7 d		
C35N	90 d	11	d
	10 t/p	4.5	d
		4.5	d
C45N	90 d	4.5	d
	10 t/p	3.2	d
		3	d
C55N	90 d	7.5	t

	10 t/p		
C30S	60 d	4	d
	40 t/p	3.5	d
		2.5	d
D15N	55 d	5.5	d
	45 t/p	4	p
	trace g	3.5	p
D25N	60 t/p	5.8	t
	40 d	5.5	p
		5.4	p
D34N	70 t/p	4	d
	30 d	3	d
		3	d
D45N	60 d	5.5	t
	40 t/p	2.7	d
		2.5	d
DD30S	88 t/p	7.5	t
	12 d	4	d
		2.7	t
E15N	85 d	10	d
	15 t/p	5	d
		4	d
E25N	90 d	8.5	d
	10 t/p	8	t
		6.3	d
E35N	65 d	5.5	t
	35 t/p	5	d
		4.5	d
E45N	70 d	4.5	d
	30 t/p	3.5	t
		3.5	d
E30S	55 d	10	d
	45 t/p	9.5	t
		5.8	d
EE25N	95 t/p	3.5	p
	5 d	3	p
		3	p

Report No. EES1-SH90-19
December 1990

F25N	95 t/p	10	d
	5 d	3.5	t
		3	d
F30N	99 t/p	7	d
	1 d	3	p
		2	p
F30S	88 t/p	5	p
	12 d	3	p
		2.5	p
FF35N	80 d	4	d
	20 t/p	4.2	p
		4	d
FF40N	60 t/p	3	d
	40 d	2.8	d
		2.7	d
FF35S	92 t/p	3.4	p
	8 d	2.5	p
		2.5	p
G25N	75 d	5.7	d
	25 t/p	6.2	v
		5.4	d
G30N	80 d	4.5	d
	20 t/p	4	d
		3.5	v
G30S	75 t/p	4.5	d
	25 d	4	d
		3.6	d
GG37S	75 d	3.2	p
	25 t/p	2.9	d
	trace o	2.6	d
H45S	65 t/p	10.4	p
	35 d	3.3	p
		3	p
HH40S	60 t/p	5.2	d
	40 d	4.5	p
		3.7	d
I35S	80 t/p	2.7	p
	20 d	2.5	d

Report No. EES1-SH90-19
December 1990

		2.6	p
J57S	95 d	7.3	d
	5 t/p	2.3	d
		1.9	v
JJ56S	50 t/p	7.7	d
	50 d	6.2	d
		6	d
K45N	98 d	3.5	d
	2 t/p	2.5	d
		2.3	d
K55N	80 d	9.5	t
	20 t/p	6	d
	trace rounded quartzite	6	d
K50S	65 d	6.2	t
	35 t/p	5.5	d
		4	d
		4	t
L61S	95 d	3.5	d
	5 t/p	3.3	d
		3.1	d
M57S	75 d	2.4	v
	25 t/p	2.3	d
		2.2	d
N61S	90 d	12.3	d
	10 t/p	8.7	d
		6.7	d
P25N	98 t/p	19	t
	2 d	2.7	t
		2.4	t
P35N	95 t/p	6	d
	5 d	4	d
		3	t
R40N	60 d	7	d
	40 t/p	6.5	d
		6.2	t
S37N	60 d	3.7	d
	40 t/p	3.5	d

Report No. EES1-SH90-19
December 1990

		3.3	d
S40N	80 t/p 20 d	5.2 2.5 2	d d d
SS40S	80 t/p 20 d	2.6 2.5 2.2	p d d
T43N	85 d 15 t/p	8.5 8 7	d d d
U45N	85 t/p 15 d	6 6 6	t t t
U50N	85 t/p 15 d	6.7 4.2 3.5	t t d
UU35S	75 t/p 25 d	4 3.3 3.3	d d d
UU45S	97 t/p 3 d	5 4.4 4 4	p p t d
V28N	70 t/p 30 d	2.1 2.1 2	t t d
W33N	60 t/p 40 d	3.3 3 2.5 2.5	d t d t
W34N	65 t/p 35 d	3 3 3 3	d t t d
Y45S	95 t/p 5 d	3 2.6 2.3	p d p
Z45N	60 d	4	d

Report No. EES1-SH90-19
December 1990

	40 t/p	3.5	t
	trace g	3	t
		3	d
ZZ45S	97 d	5.7	d
	3 t/p	4.8	d
		3.7	d
a55N	60 d	7.2	d
	40 t/p	6.3	d
		5	d
b58N	80 d	6.3	d
	20 t/p	4	d
		2.7	d
g55N	90 d	14	d
	10 t/p	13.5	d
		10.4	d
t59N	65 t/p	29	d
	35 d	6	t
		4.5	d
x57N	85 d	11.4	t
	15 t/p	6.3	d
		6	t

PART 3: PALEOCURRENT DATA

Flow directions were measured from pebble imbrications, cross bed dips in fluvial units, and channel orientations. Strike and dip of cross beds give flow directions at right angles to the strike in the dip direction. Azimuth and plunge give flow directions down dip towards the azimuth. Data of Manley are already reduced to flow directions, regardless of structures measured. All data, reduced to flow directions, are shown in Figure 4. Locations of measurements are given per the convention discussed in the section on Methods.

By Manley:

Unit C. Channel cross bedding.

LOCATION	FLOW DIRECTION
1. N25H2.3V	S5E
2. N35H2.9V	S55E

Unit E. Pebble imbrication.

LOCATION	FLOW DIRECTION
1. N14.3H3V	S60E
2. N15H 3V	OE
3. N15H 2.6V	S70E
4. N16.6H2.5V	S25E
5. N24H 3.3V	S65E
6. N28H 3.6V	OE
7. N29.4H3.3V	S65E
8. N33H 3.5V	S22E
9. N35.4H3.4V	S15E
10. N36H 3.5V	S30E
11. N43.7H3.6V	S85E
12. N50H 3.8V	S30E
13. S25.9H3.8V	S15E
14. N26H 3.9V	S25E

Channel cross bedding.

LOCATION	FLOW DIRECTION
1. N19.3H3.3V	S82W
2. N19.6H3.3V	S20E
3. N26H 3.5V	S25E

By Gardner and Baron:

Location/unit structure measurement (s&d=strike and dip, az&p=azimuth and
plunge)

N7H/C	cross bed	s & d: N56E,10SE
S12H/E	channel	az & p: N68E,11NE
N14H/E	cross bed	s & d: N54E,14SE
S15.5H/E	channel	az & p: N70E, 8 NE
N18H/E	cross bed	s & d: N10W, 21NE
N18H/E	cross bed	s & d: N19E,17SE
S24H/E	channel	az & p:N80E,20NE
S30H/E	channel	az & p: N36E, 17NE
N30H/E	channel	az & p: N70E, 14NE
S25H/E	cross bed	s & d: N2E, 11E
S28.75H/G	foreset bed	s & d: N9W, 24E
N42H/E	channel	az & p: S8E, 20SE
N42H/E	cross bed	s & d: N64E, 11 SE
N44H/Z	cross bed	s & d: N3E, 12E
N44H/Z	cross bed	s & d: N-S, 7E
N45H/K	cross bed	s & d: N60E, 14SE
N45H/K	cross bed	s & d: N54E, 5SE
S48.5H/ZZ	channel	az & p: S12E, 23SE
S50.5H/K	cross bed	s & d: N8E, 10SW
S60H/N	channel	az & p: S15E, 11SE

TABLE 1. ^{14}C dates. All analyses on charcoal; unless otherwise indicated, single pieces were analyzed. Dates are reported as radiocarbon years before 1950 A.D. See Plate 2 for unit designations and sample locations. AMS = Accelerator Mass Spectrometry. Analytical laboratory sample numbers are also shown. (see discussion of ^{14}C dating in METHODS section.)

Sample No.	Unit	Date	Technique/Comments
SHT-1-10A (Beta-26084) (ETH-4139)	UU	2840 \pm 75	AMS
SHT-1-10B (Beta-26085)	UU	2970 \pm 100	Extended Beta counting
SHT-1-15B (Beta-26086)	HH	3800 \pm 100	Beta counting
SHT-1-18 (Beta-26087)	B	300 \pm 70	Beta counting
SHT-1-19 (Beta-26088) (ETH-4140)	SS	4240 \pm 80	AMS/composite sample
SHT-1-20 (Beta-26089) (ETH-4160)	P	3495 \pm 70	AMS/composite sample
SHT-1-21 (Beta-26090)	S	3600 \pm 170	Extended Beta counting/composite
SHT-1-22 (Beta-26091)	D	1610 \pm 160	Extended Beta counting/composite
SHT-1-23 (Beta-26092)	Y	5690 \pm 250	Extended Beta counting
SHT-1-26D (Beta-28720)	K	3730 \pm 90	Beta counting

FIGURES:

Figure 1: Map of north-central Rio Grande rift showing major rift basins, sedimentary rift-fill deposits (horizontal dash), Precambrian rocks (random dash), and Tertiary to Quaternary volcanic rocks (fine stipple). Major fault systems are shown schematically. LA, SF, and A are Los Alamos, Santa Fe, and Albuquerque, respectively. (modified from Gardner and Goff, 1984)

Figure 2: Pajarito fault system segmentation in Los Alamos County vicinity. Delineation of fault segmentation is based on current understanding of ages and histories of movements, Quaternary slip rates, style of deformation, and geometric relations. Site of trench SHT-1 is shown on the Guaje Mountain fault segment.

Figure 3: Detailed map of SHT-1 and vicinity showing nearby natural exposure of fault in Cabra Canyon, positions of auger holes (stars with CC numbers), and current main drainage channels. For reference, a number of spatial control points are shown (dots), and main fault traces and major subsidiary faults are shown approximately.

Figure 4: Sketch of natural exposure of main fault in outcrop about 70 meters north of SHT-1. See Figure 3 ("outcrop of fault trace") for location of this figure.

Figure 5: Paleocurrent data: flow directions for unit E unless otherwise indicated; flow directions for unit G may have been affected by drag on the mid-trench strike slip zone. Main fault traces and major subsidiary faults shown approximately.

Figure 6: Lower hemisphere stereonet plots of directions of magnetization components isolated by alternating field demagnetization in samples of the lacustrine units of the slit trench. Upper plot is tilt corrected with the dip of the units rotated to horizontal. Lower plot is not tilt corrected. Directions indicate reversed polarity.

Figure 7: Lower hemisphere stereonet (Schmidt) plots of poles to planes of main faults (solid dots), subsidiary faults (open circles), and fractures (triangles) of the main fault zone. Also shown are strike lines of the faults at the equator of the sphere. Figure 7a is for older portion of main fault zone; Figure 7b is for younger portion of main fault zone.

Figure 8: Lower hemisphere stereonet plot of faults and fractures of the mid-trench low angle fault.

Figure 9: Lower hemisphere stereonet plot of faults and fractures of the mid-trench strike slip zone.

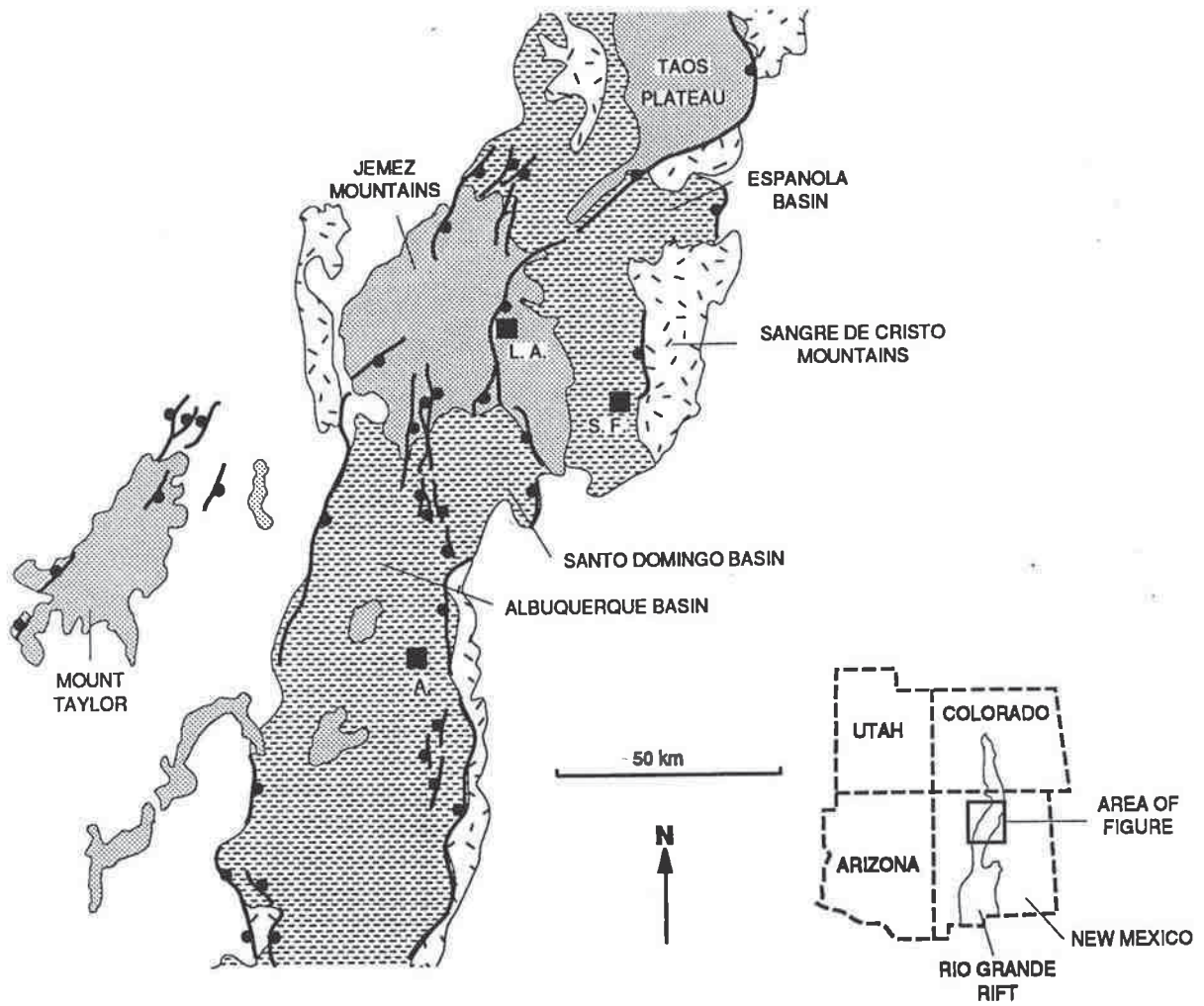


Figure 1

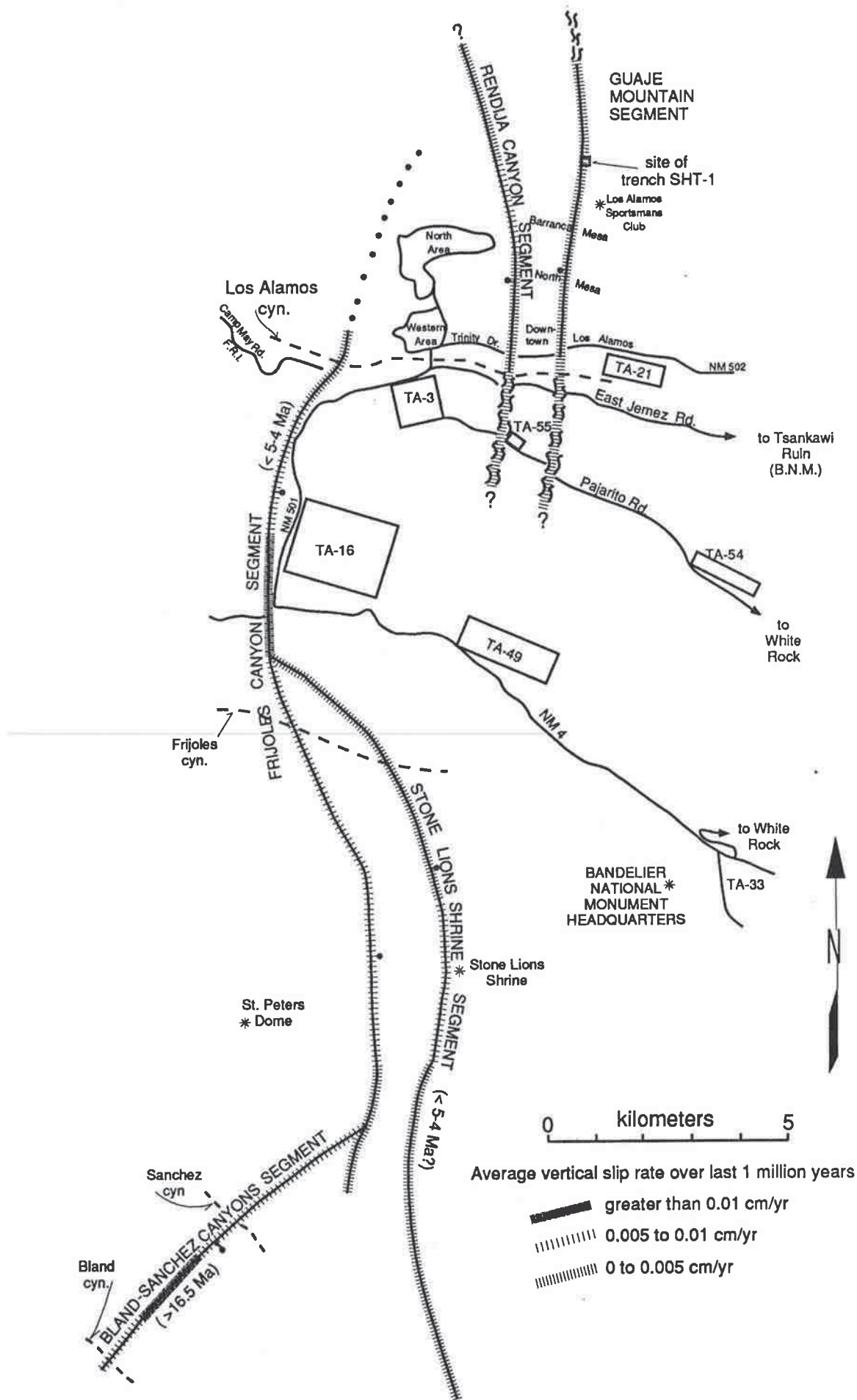


Figure 2

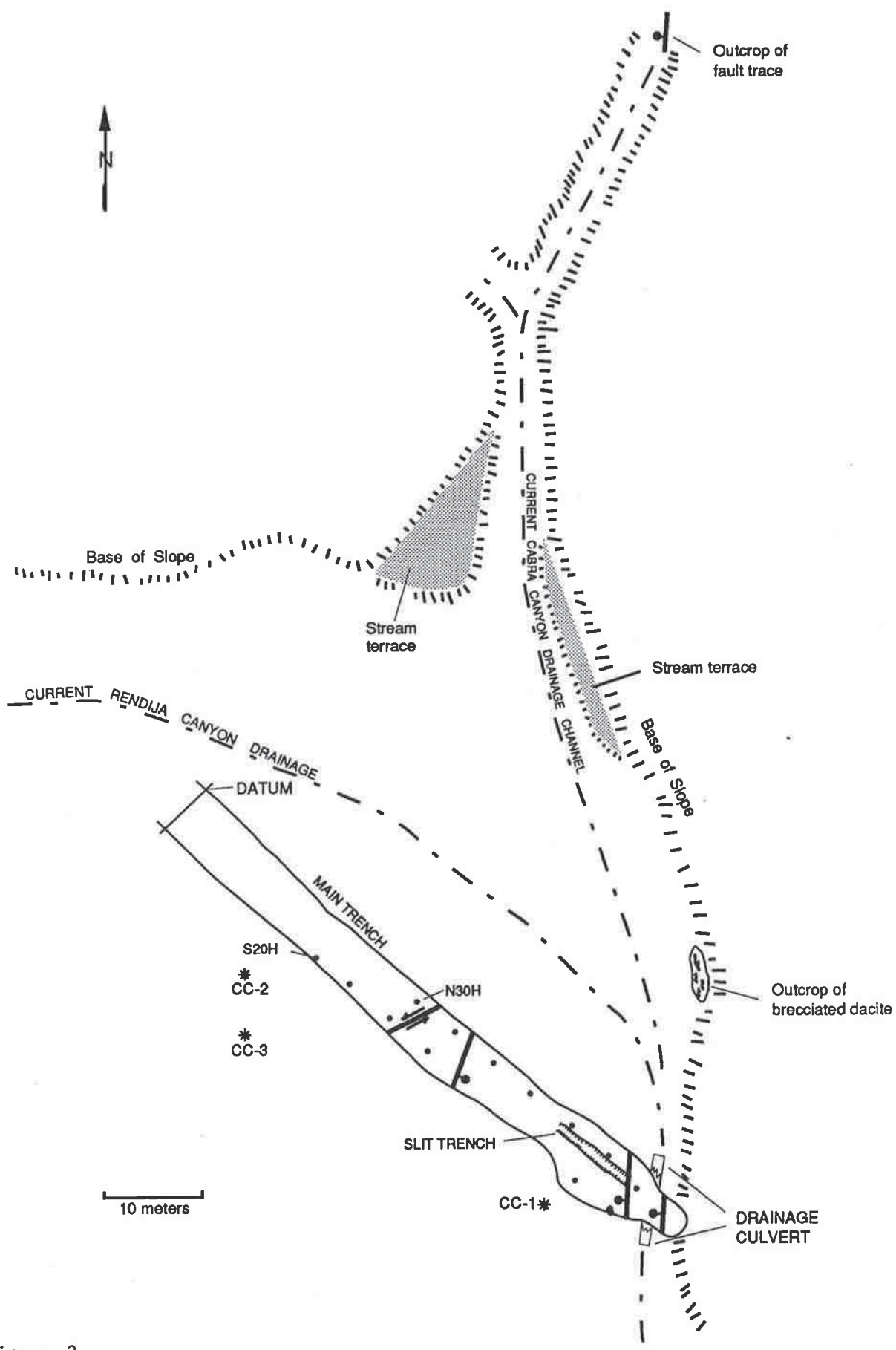


Figure 3

N86W

S86E

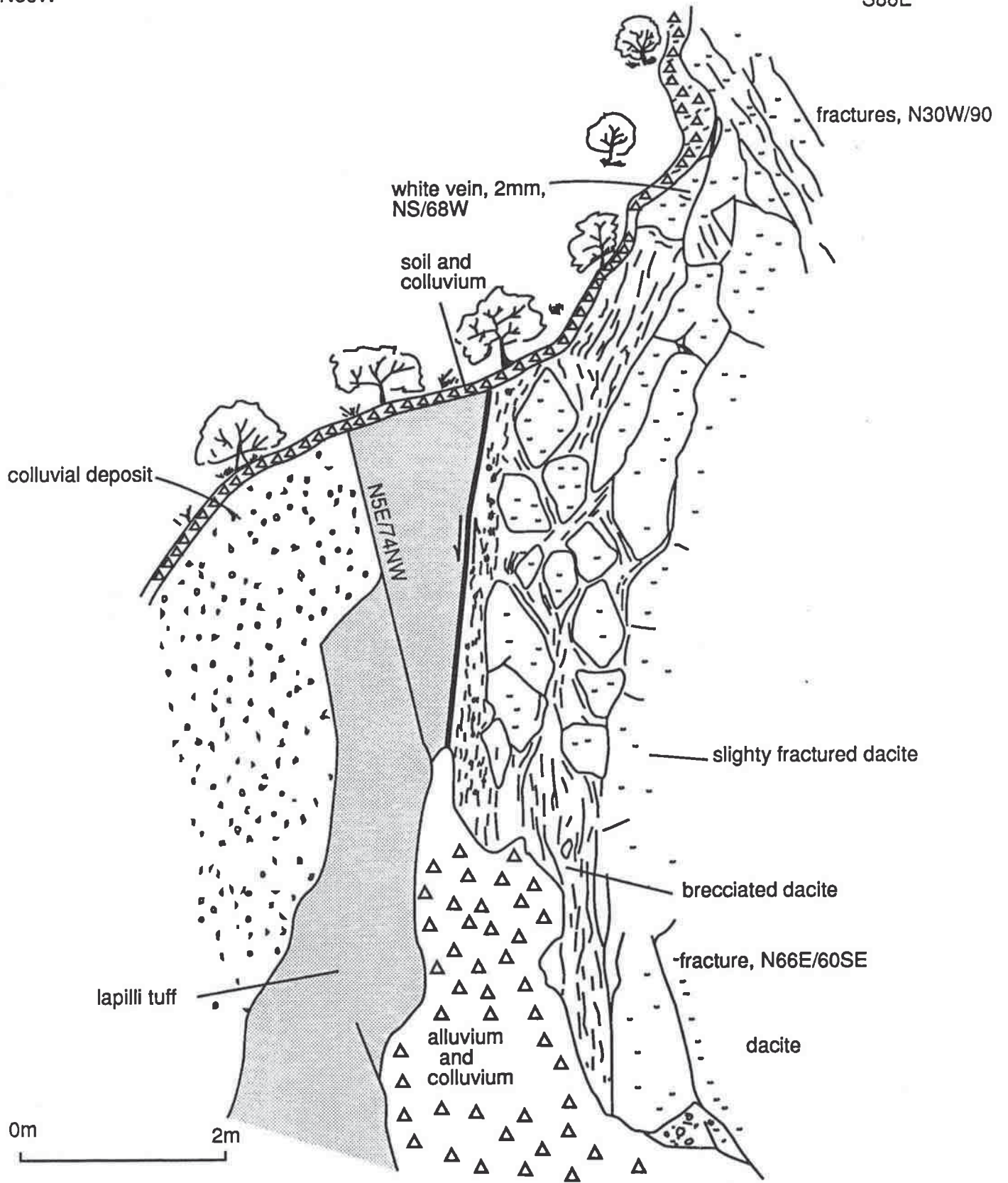


Figure 4

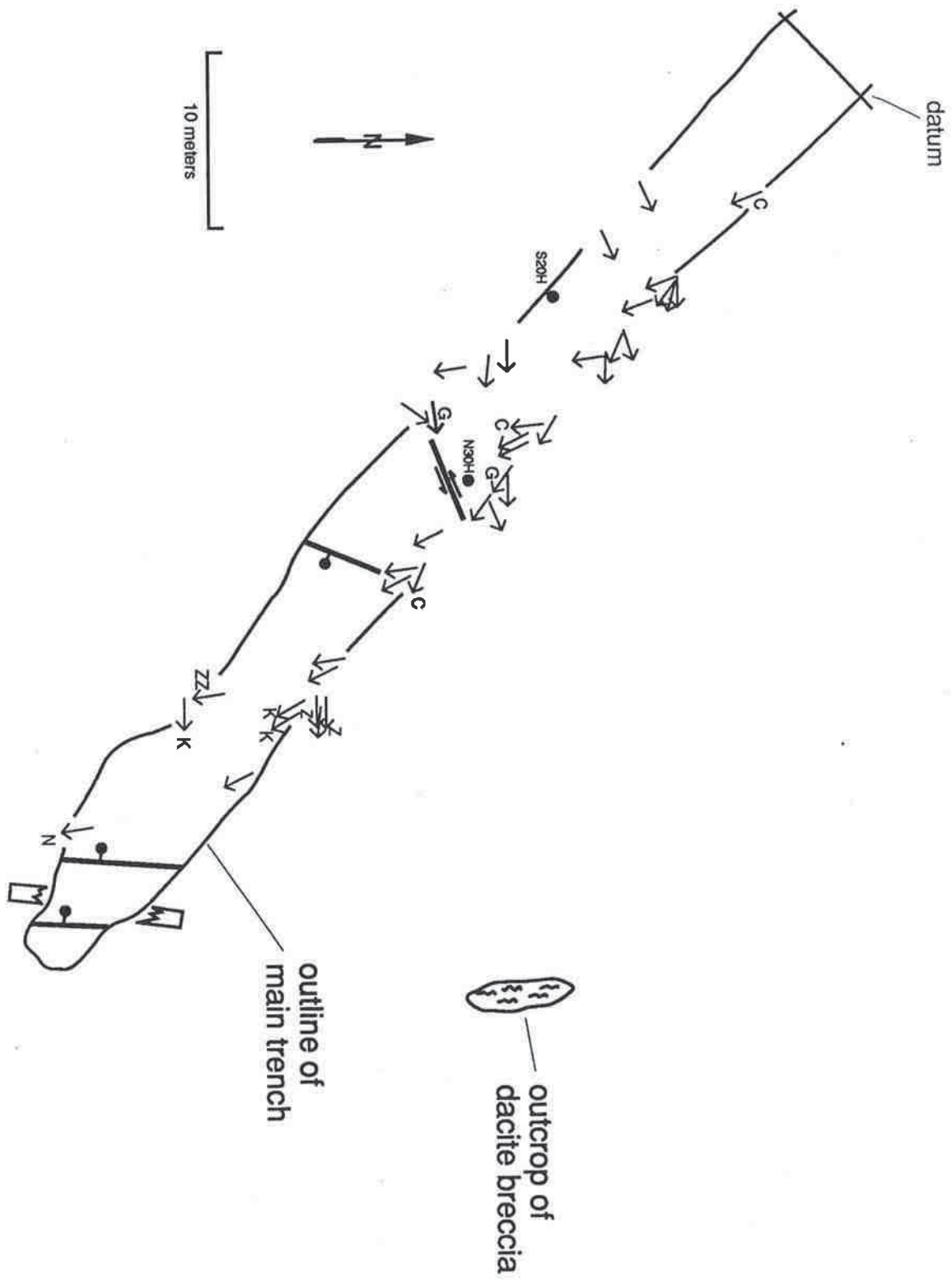
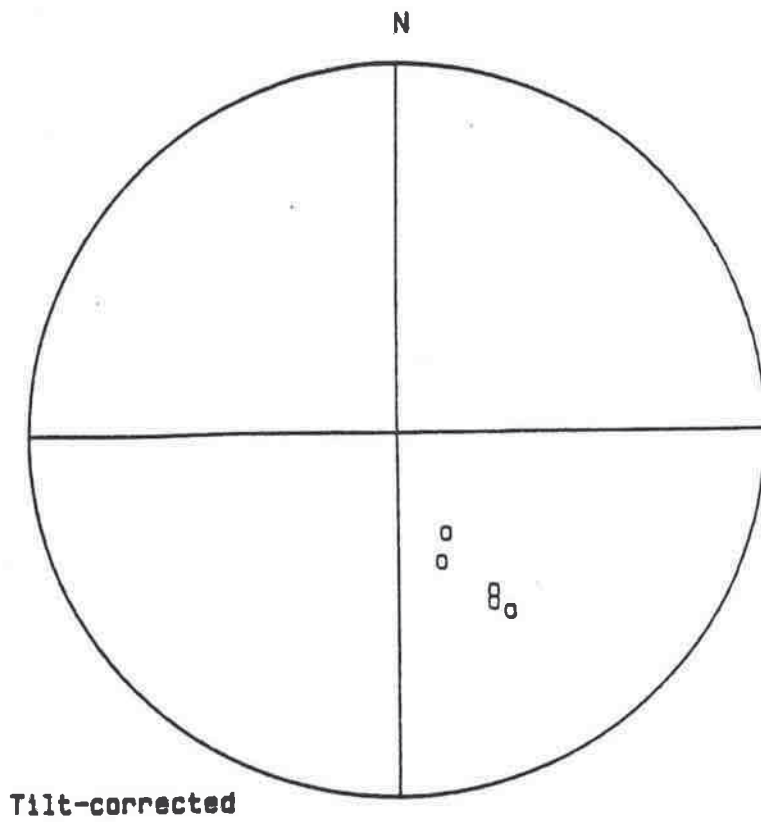
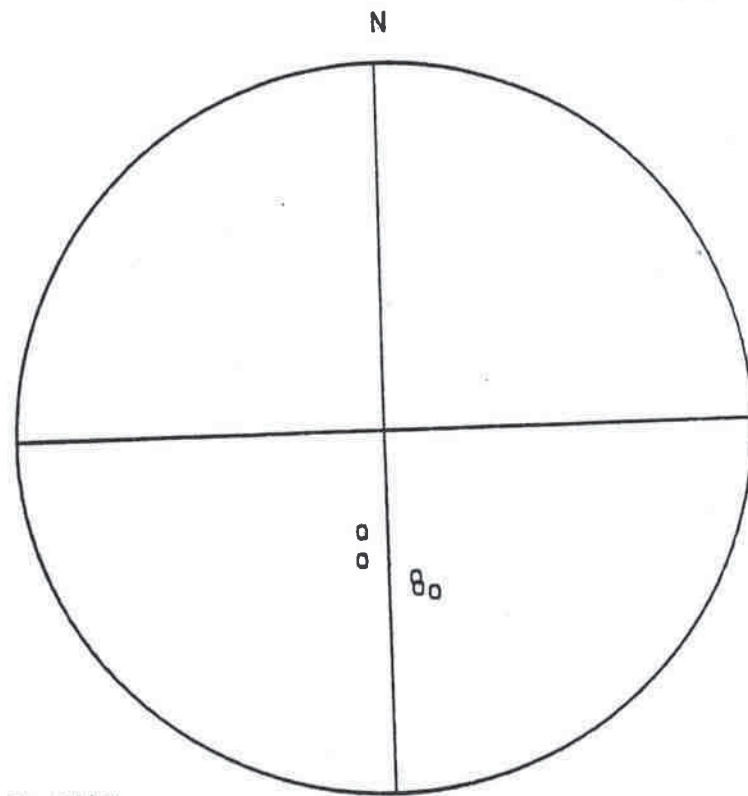


Figure 5

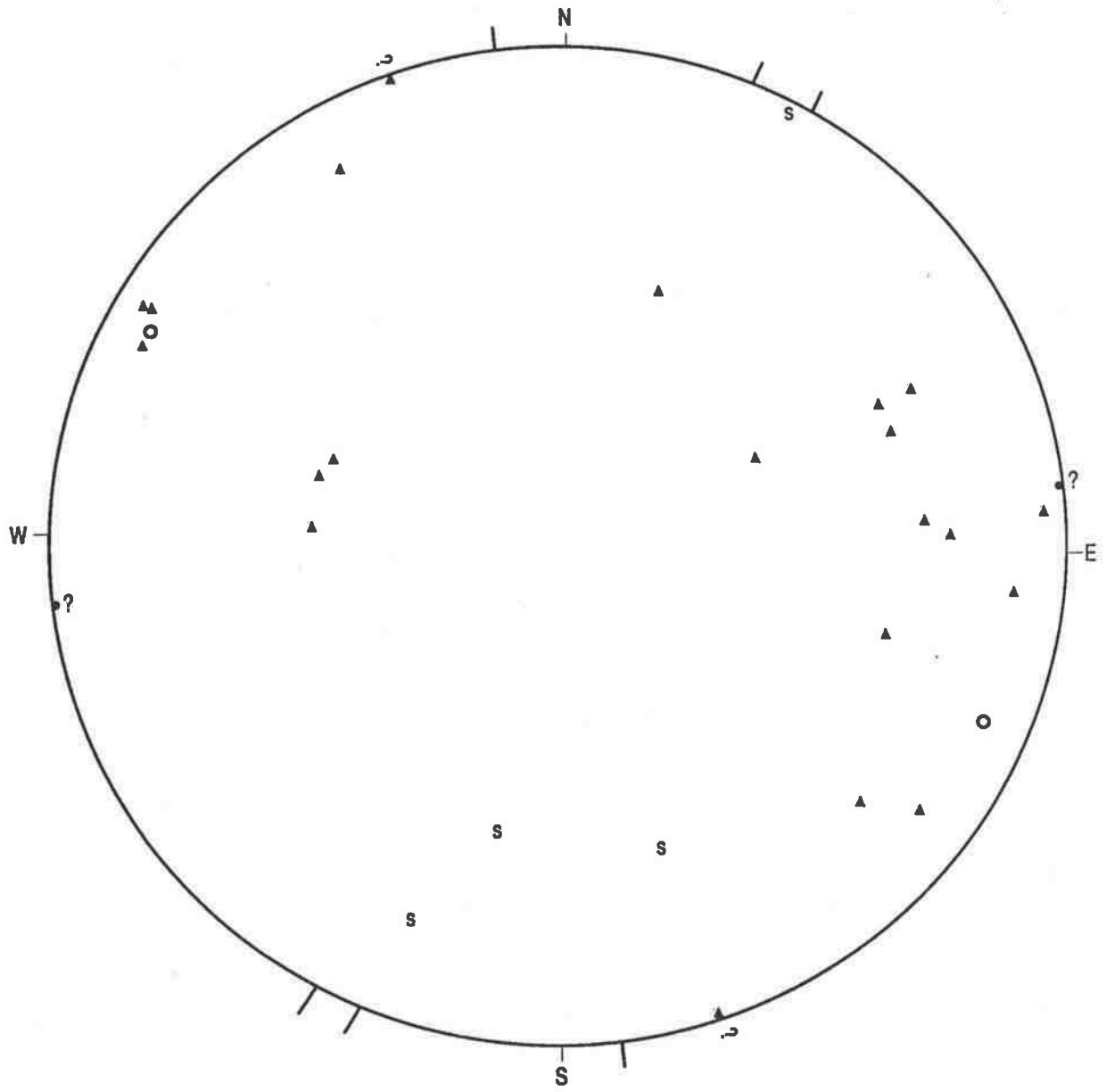


Tilt-corrected



In-Situ

Figure 6



Older portion of
main fault zone

- = faults
- = subsidiary faults
- ▲ = fractures
- s = slickensides
- ? = pole to vertical plane

Figure 7a

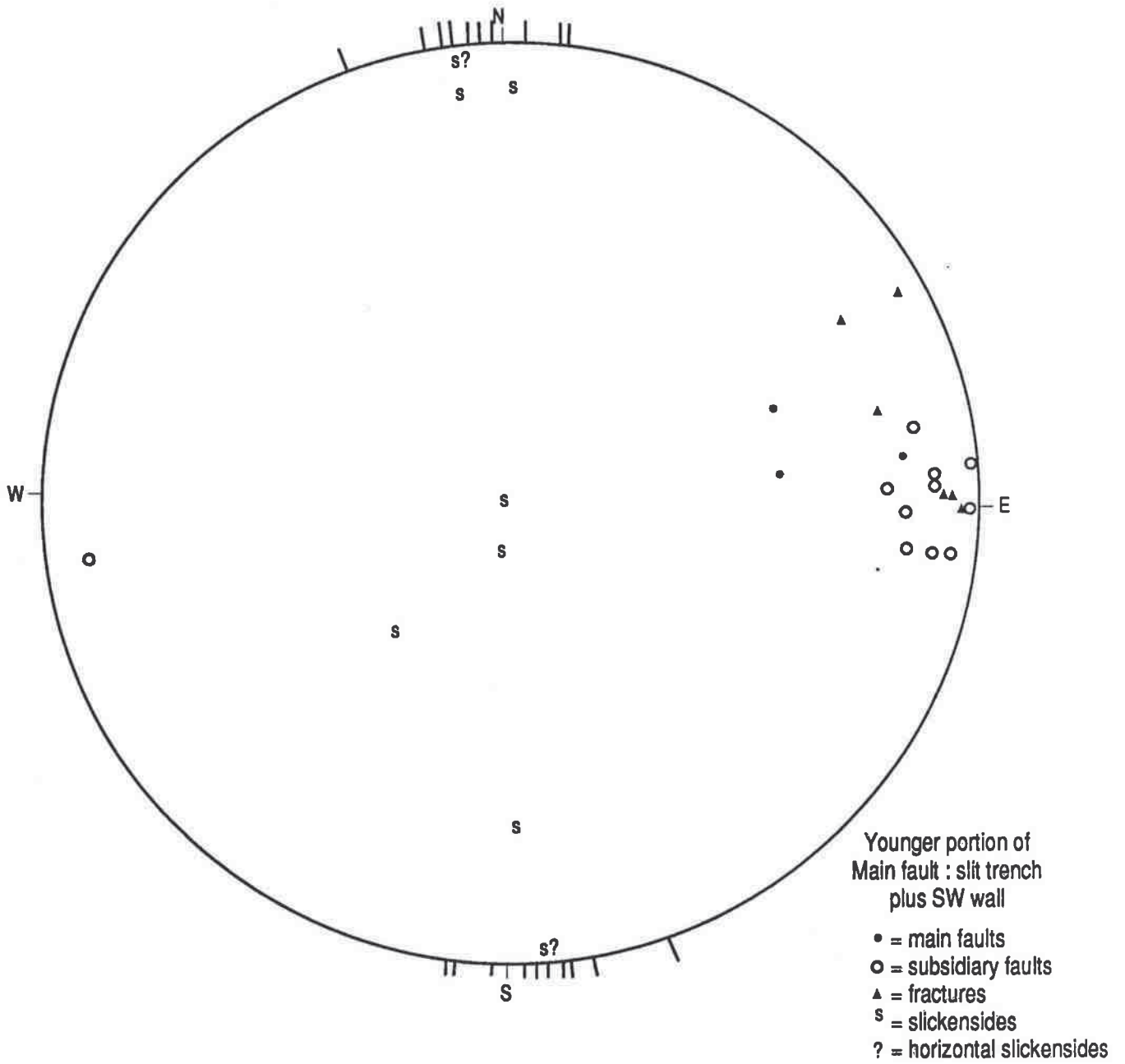


Figure 7b

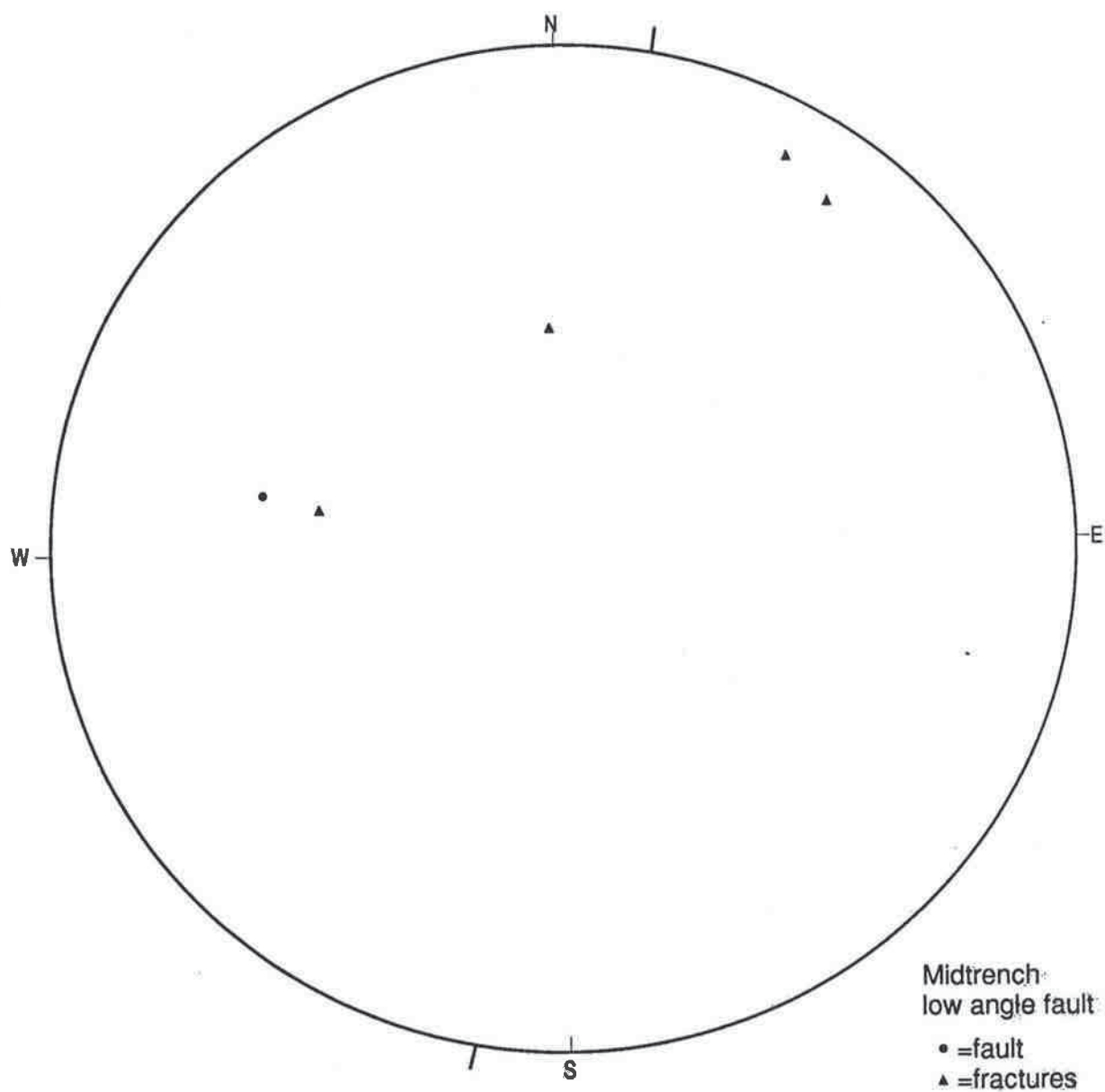


Figure 8

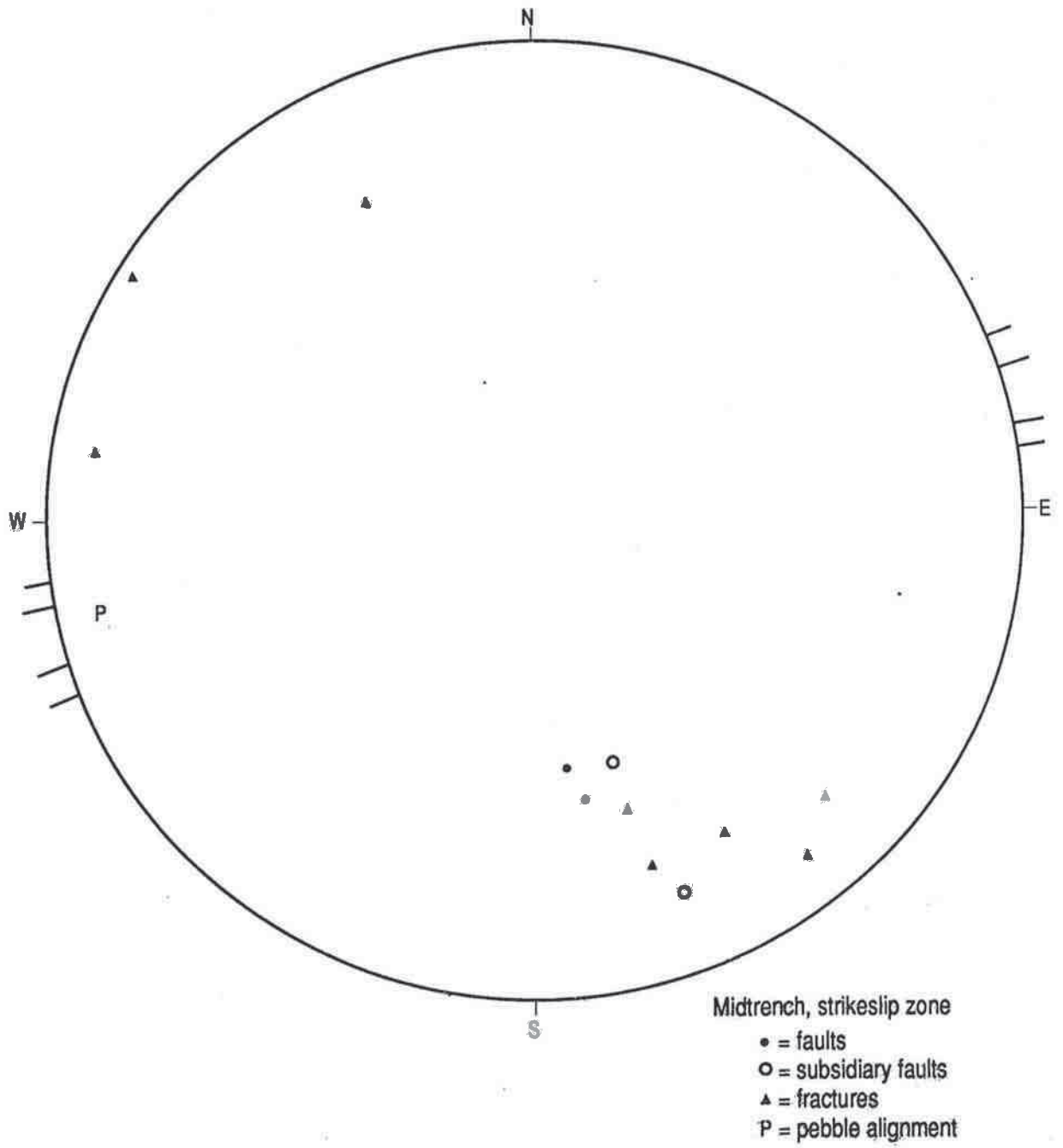


Figure 9

EXPLANATION OF PLATE SYMBOLS



=

FAULT, ARROWS
INDICATE VERTICAL MOVEMENT



=

FRACTURE



=

CONTACT



=

GRADATIONAL CONTACT; SOME SYMBOLS DASHED WHERE APPROXIMATE



=

INTENSE SHEARING/BRECCIATION



=

GOUGE



=

STRIKE SLIP MOVEMENT OUT OF PLANE OF FIGURE



=

STRIKE SLIP MOVEMENT INTO PLANE OF FIGURE

S & D

=

STRIKE AND DIP

AD

=

APPARENT DIP

S. S.

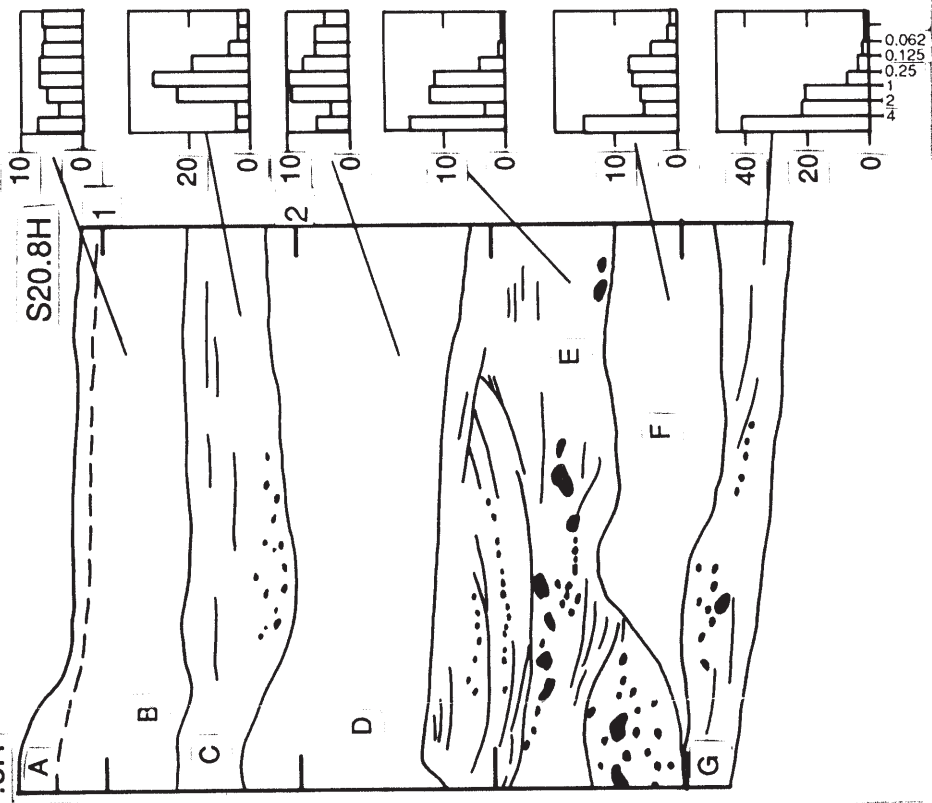
=

TREND AND PLUNGE OF SLICKENSIDES

CC-3

WEIG

S17.8H



Fine to v. coarse sandy loam to loamy sd.; <5% 2-16 mm

Loamy fine to v. coarse sd.; <5% 2-16 mm
Same as above, less loamy

Fine to v. coarse loamy sand <5% 2-64 mm

Fine to v. coarse sd.; <5% 2-64 mm

Same as above; 10-15% 2-64 mm

Same as above; 15-20% 2-64 mm

Sharp, poss. unconformable contact
Loamy fine to coarse sand; 5-10% 4-16 mm; some to 25 mm

Same as above; <5% 4-16 mm
As above; 5-15% 4-32 mm

As above; <5% 4-32 mm

Pebble gravel layer

As above; 5-10% 4-32 mm

As above; <5% 4-32 mm

Units as above; thin bedded, alternating 5-10% pebbles and <5% pebbles in pumiceous sand

As above; 5-10% pebbles

As above; <5% pebbles

Fine to coarse sd.; few 2-8 mm
Loamy sd. to sd.; 10-15% 4-32 mm

As above, sd. to loamy sd.; 5-10% 4-32 mm

As above; sand & loamy sand; <5% 4-32 mm

As above, loamy sand; <5% 4-32 mm slightly redder than above

Grain Size (mm)

Grain Size (mm)

Loamy fine to v. coarse
Fine to v. coars
Fine to v. coars
Fine to v. coars
As above; char
Fine to v. coars
5-10% 2-16 mm
medium to v. co
sd; 10% 2-16 m
Fine to v. coars
As above, to lo
Fine to v. coars
coarse pebble l

ATE 8

+

+

+

+

+

FLOOR OF MAIN TRENCH

MID-TRENCH
LOW ANGLE
FAULT

SOUTHWEST WALL

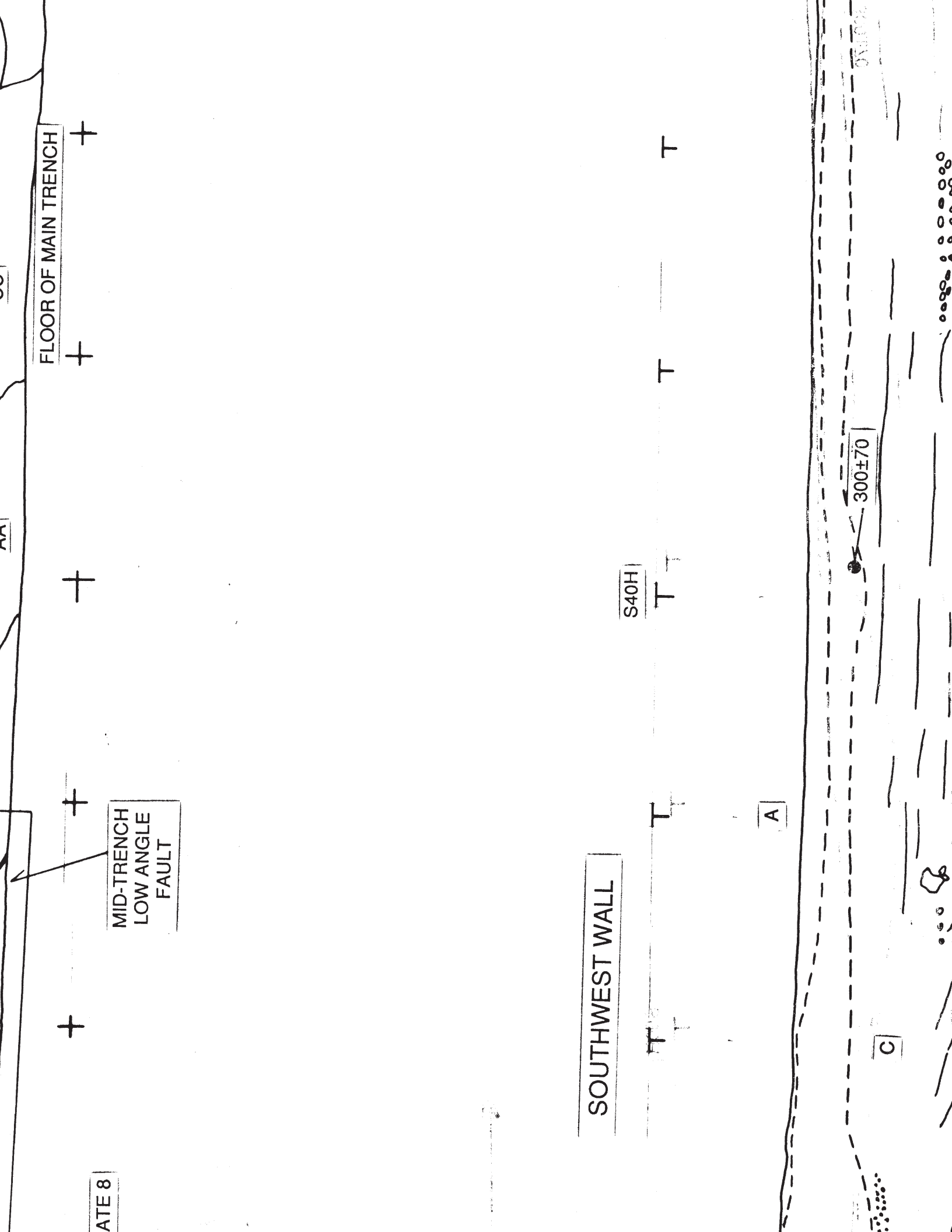
S40H

A

C

300±70

0.0000



brecciated
colluvium
II

brecciated
dacite

sheared
dacite

sheared
dacite

erosional contact

dacite
clast

dacite
clasts

N27E, 80

S.S. N9W, 11N

S.S. N5E, 82S

N9W, 74W

N15W, 70W

Unit K

colluvium II

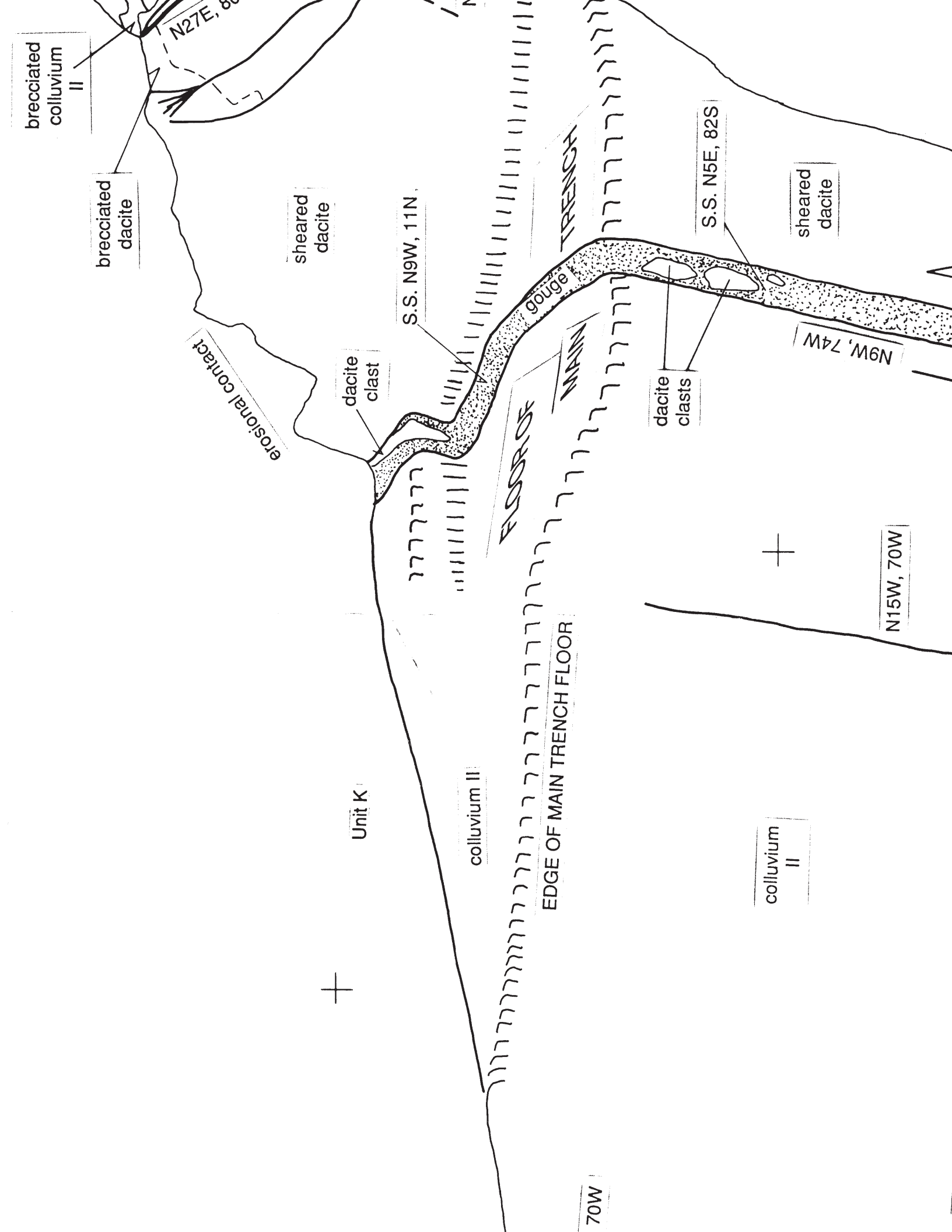
colluvium
II

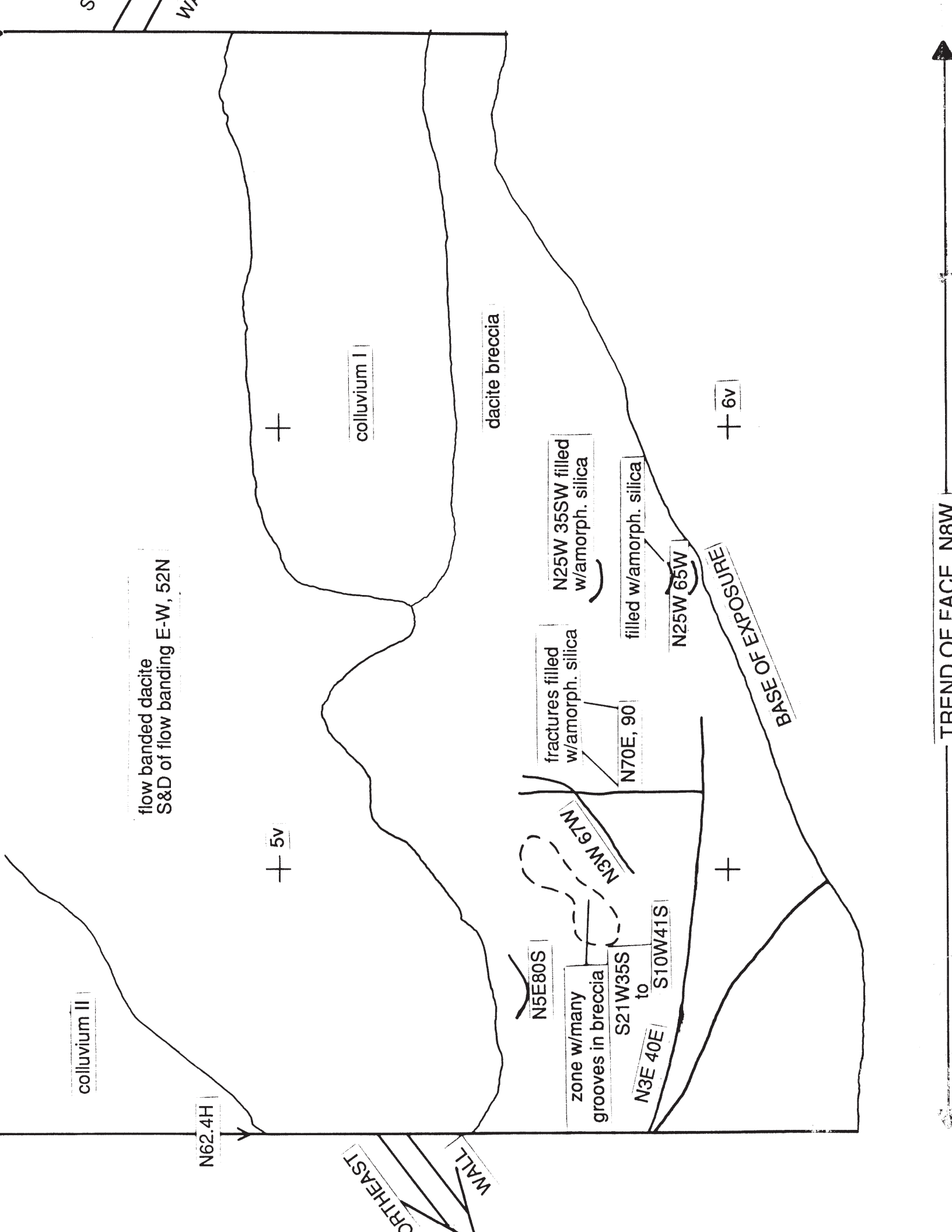
EDGE OF MAIN TRENCH FLOOR

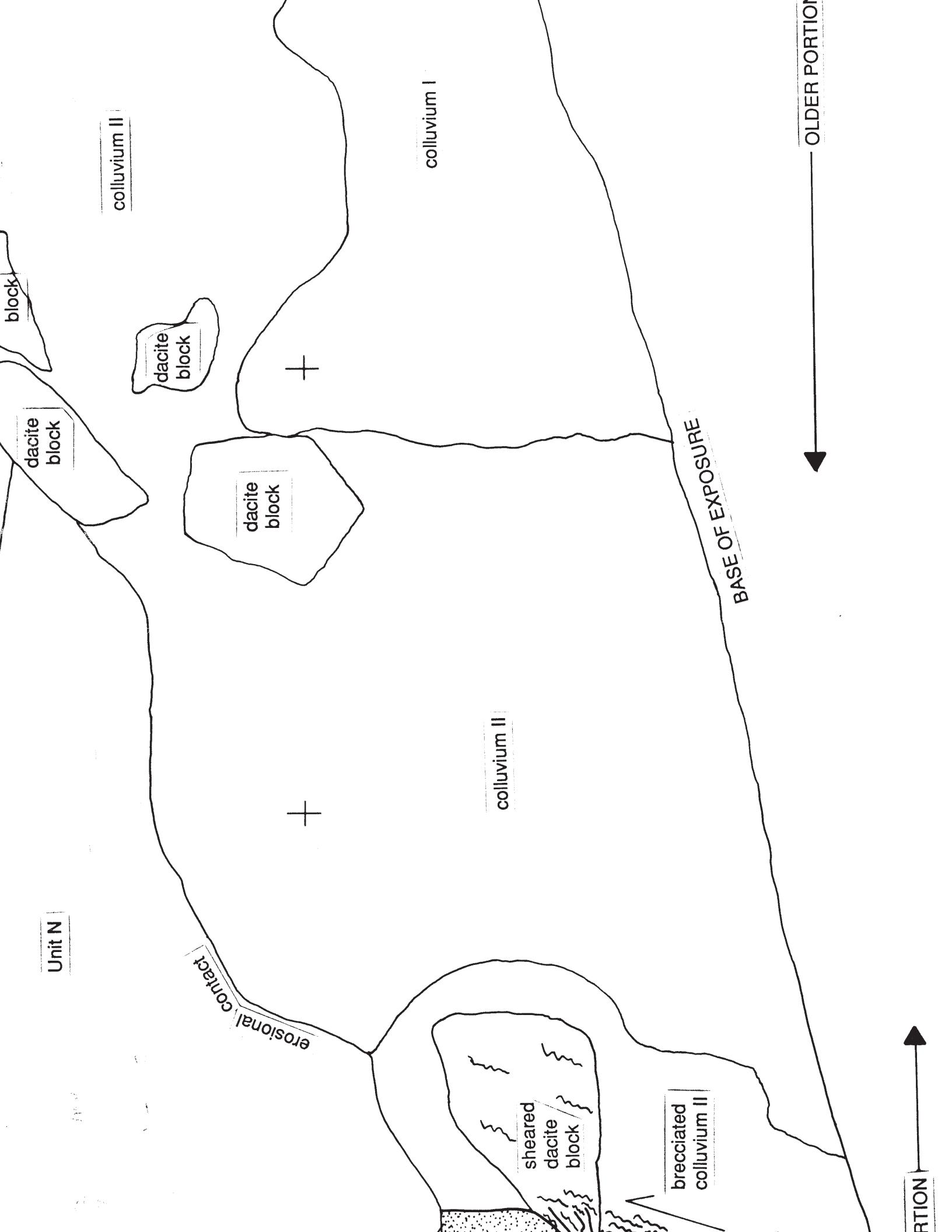
FLOOR OF
MAIN
TRENCH

gouge

70W







1
7v

erosional contact

Unit K

covered

SS. 90

SS. 0

block of non-welded lapilli tuff, pumice clasts to
4 cm, moderately lithified

7v

+

colluvium II

N54H

+ 7v

dacite blocks



COVERED W/SPOIL HEAP

very red, sandy lithified block of colluvium (?)

Unit K

matrix supported gravel

colluvium II ?

graded coarse to silt arkosic arenite w/pumice clasts about 0.5 cm

graded ark. arenite

7v

N50H

FLOOR OF TRENCH

breccia to gouge of pumiceous material

N51H

N52H

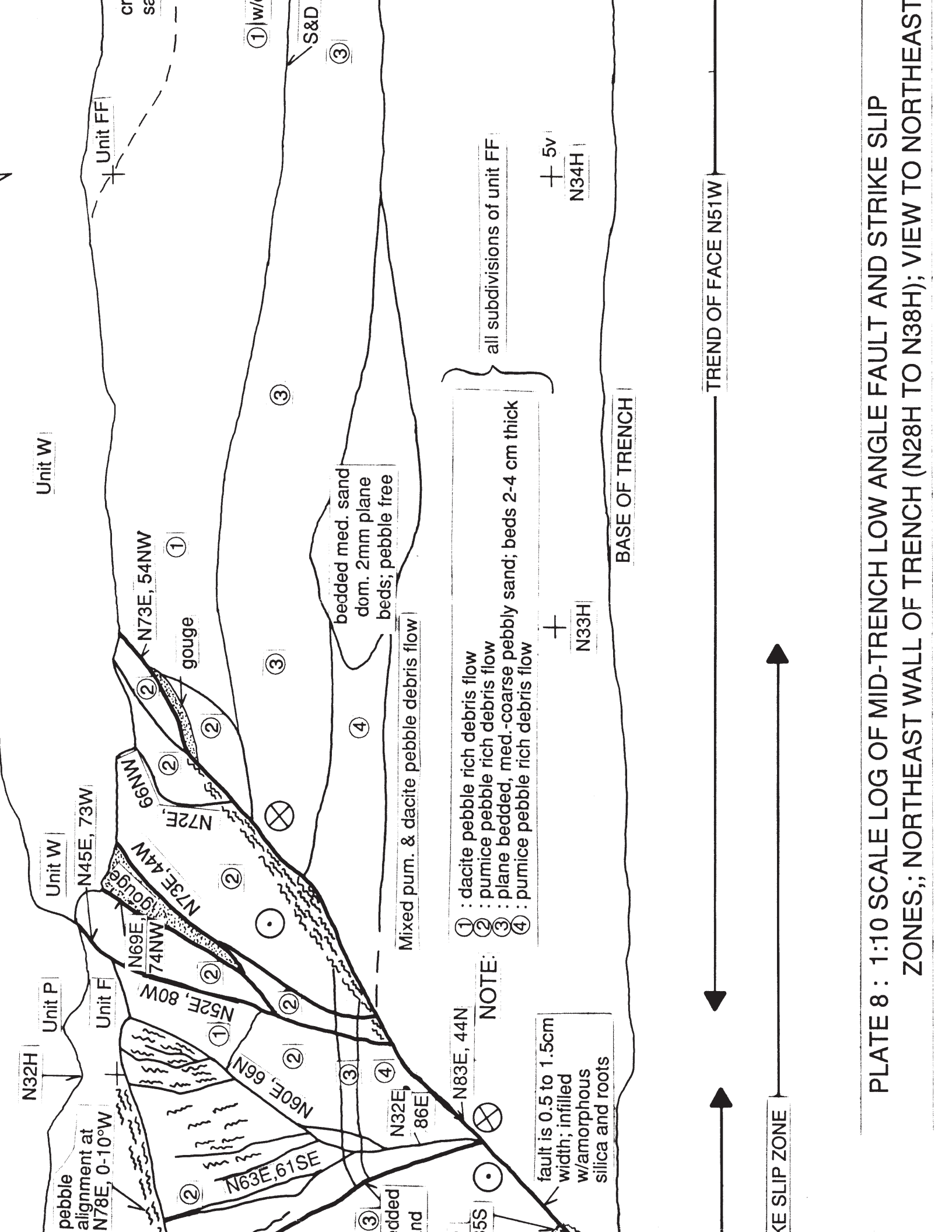


PLATE 8 : 1:10 SCALE LOG OF MID-TRENCH LOW ANGLE FAULT AND STRIKE SLIP ZONES; NORTHEAST WALL OF TRENCH (N28H TO N38H); VIEW TO NORTHEAST

